Biochemistry and Chemical Biology
Microbiology and Infectious Disease

2-oxoglutarate triggers assembly of active dodecameric *Methanosarcina mazei* glutamine synthetase

Reviewed Preprint
v2 • February 17, 2025
Revised by authors

Reviewed Preprint
v1 • May 28, 2024

Eva Herdering, Tristan Reif-Trauttmansdorff, Anuj Kumar, Tim Habenicht, Georg Hochberg, Stefan Bohn, Jan Schuller, Ruth A Schmitz

Institute for General Microbiology, Christian Albrechts University, Kiel, Germany • Center for Synthetic Microbiology (SYNMIKRO) Research Center and Department of Chemistry, Philipps-Universität Marburg, Marburg, Germany • Evolutionary Biochemistry Group, Max Planck Institute for Terrestrial Microbiology, Marburg, Germany • Department of Chemistry, Philipps-Universität Marburg, Marburg, Germany • Cryo-Electron Microscopy Platform and Institute of Structural Biology, Helmholtz Munich, Neuherberg, Germany

eLife Assessment

This study reveals a novel mechanism of glutamine synthetase (GS) regulation in Methanosarcina mazei, demonstrating that 2-oxoglutarate (2-OG) directly promotes GS activity by stabilizing its dodecameric assembly. Using mass photometry, activity assays, and cryo-electron microscopy, the authors show that GS transitions from a dimeric, inactive form at low 2-OG concentrations to a fully active dodecameric complex at saturating 2-OG levels, highlighting 2-OG as a key effector in C/N sensing. The findings are **valuable**, supported by **solid** data, and provide new insights into archaeal GS regulation, though further clarification of interactions with known partners like Glnk1 and sp26 is needed.

https://doi.org/10.7554/eLife.97484.2.sa4

Abstract

Glutamine synthetases (GS) are central enzymes essential for the nitrogen metabolism across all domains of life. Consequently, they have been extensively studied for more than half a century. Based on the ATP dependent ammonium assimilation generating glutamine, GS expression and activity are strictly regulated in all organisms. In the methanogenic archaeon *Methanosarcina mazei*, it has been shown that the metabolite 2-oxoglutarate (2-OG) directly induces the GS activity. Besides, modulation of the activity by interaction with small proteins ($GlnK_1$ and sP26) has been reported. Here, we show that the strong activation of *M. mazei* GS ($GlnA_1$) by 2-OG is based on the 2-OG dependent dodecamer assembly of $GlnA_1$ by using mass photometry (MP) and single particle cryo-electron microscopy (cryo-EM) analysis of purified strep-tagged $GlnA_1$. The dodecamer assembly from dimers occurred without any detectable intermediate oligomeric state and was not affected in the presence of $GlnK_1$. The 2.39 Å cryo-EM structure of the dodecameric complex in the presence of 12.5 mM 2-OG demonstrated that 2-OG is binding between two monomers. Thereby, 2-OG appears to induce the dodecameric

assembly in a cooperative way. Furthermore, the active site is primed by an allosteric interaction cascade caused by 2-OG-binding towards an adaption of an open active state conformation. In the presence of additional glutamine, strong feedback inhibition of GS activity was observed. Since glutamine dependent disassembly of the dodecamer was excluded by MP, feedback inhibition most likely relies on an allosteric binding of glutamine to the catalytic site.

Based on our findings, we propose that under nitrogen limitation the induction of *M. mazei* GS into a catalytically active dodecamer is not affected by $GlnK_1$ and crucially depends on the presence of 2-OG.

Introduction

Nitrogen is one of the key elements in life and it is essentially required in the form of ammonium for biomolecules such as proteins or nucleic acids. Two major pathways of ammonium assimilation in bacteria and archaea are known. Under nitrogen (N) sufficiency, glutamate dehydrogenase (GDH) is active and generates glutamate from 2-oxoglutarate (2-OG) and ammonium (reviewed in van Heeswijk et al., 2013). Under N limitation however, low ammonium concentrations lead to an inactive GDH as a result of its low ammonium affinity, whereas the expression of glutamine synthetase (GS) is strongly induced in response to N limitation (Bolay et al., 2018; Gunka and Commichau, 2012; Stadtman, 2001). Consequently, under low ammonium conditions, GS together with glutamate synthase (GOGAT) are responsible for ammonium assimilation via the GS/GOGAT pathway, one of the major intersections in central carbon and N metabolism. Accordingly, GS present across all domains of life plays a central role in cellular N assimilation under low N availability. The enzyme, its structure and regulation have been investigated in detail in different organisms for more than half a century (e.g. Dos Santos Moreira et al., 2019; Stadtman, 2001; Woolfolk and Stadtman, 1967).

Most of the GS are grouped into three major classes based on their monomeric size and oligomerization properties (overview in Dos Santos Moreira et al., 2019). GSI and GSIII, both found in bacteria and archaea, mostly form dodecamers, whereas GSII found in Eukaryotes form decamers of smaller subunits (Dos Santos Moreira et al., 2019; He et al., 2009; Valentine et al., 1968; van Rooyen et al., 2011). The GSI class can be further grouped into Iα-type GS and Iβ-type GS based on their amino acid sequence and respective molecular mechanisms of activity regulation. Iß-type GS contain a conserved adenylylation site (Tyr397 residue near the active site), that allows for covalent modification of Iβ-type GS and leads to inactivation of the enzyme (Brown et al., 1994; Magasanik, 1993; Shapiro and Stadtman, 1970). Iα-type GS on the other hand are not covalently modified and mainly show feedback inhibition by end products of the glutamine metabolism, including glutamine (Fisher, 1999; Gunka and Commichau, 2012).

GS regulation on transcriptional level

Since in contrast to GDH, GS catalyzed generation of glutamine requires ATP, most organisms strictly regulate the expression of GS in response to the nitrogen availability on the transcriptional level. In gram negative bacteria, mainly transcriptional activation of the coding gene (*glnA*) under low nitrogen availability occurs via a transcriptional activator (e.g. NtrC in *Escherichia coli* (Jiang et al., 1998)). For several gram positive bacteria however, the mechanism of regulation is a de-repression of *glnA* transcription under N limitation, which has also been shown for methanoarchaea (Cohen-Kupiec et al., 1999; Fedorova et al., 2013; Fisher, 1999; Fisher and Wray, 2008; Hauf et al., 2016; Weidenbach et al., 2010, 2008). Whereas in gram positives the signal perception is complex and often also involves protein interactions of GS with transcriptional regulators (reviewed in Gunka and Commichau, 2012), signal perception and transduction in methanoarchaea occurs directly via the small effector molecule 2-OG, which

increases under N limitation. It has been shown that binding of 2-OG to the global N repressor protein NrpR significantly changes the repressor conformation resulting in dissociation from its respective operator (Lie et al., 2007; Weidenbach et al., 2010; Wisedchaisri et al., 2010). In addition to expression regulation, the activity of GS is also strictly regulated in all organisms in response to changing N availabilities, however the underlying molecular mechanism(s) of inhibition significantly differ for the various GS classes and in various organisms (Reitzer, 2003).

Regulation of GS activity: highly diverse and often complex in various organisms

An extensive repertoire of cellular control mechanisms regulating GS activity in response to N availability has been observed in different organisms. Inhibitory mechanisms in response to an N upshift range from feedback inhibition by e.g. glutamine or other end products of the glutamine metabolism (e.g. *E. coli* (Stadtman, 2004), *Bacillus subtilis* (Deuel et al., 1970), yeast (Legrain et al., 1982)), proteolytic degradation (yeast, (Legrain et al., 1982)), covalent modification by adenylylation of the 1ß-type GS subunits (e.g. enterobacteriaceae), thiol-based GS regulation (e.g. in soybean nodules (Masalkar and Roberts, 2015)), inhibition by regulatory proteins (e.g. in gram positive bacteria (Travis et al., 2022a)), inhibition by interactions with small proteins (e.g. inhibitory factors in Cyanobacteria (García-Domínguez et al., 1999; Klähn et al., 2018, 2015)), to directly effecting the activity through the presence or absence of the small metabolite 2-OG, which has been shown for the first time for *Methanosarcina mazei* (Ehlers et al., 2005). Moreover, often several of the different regulatory mechanisms for GS activity are reported for one organism. For example, yeast GS (ScGS) is regulated via feedback inhibition by glutamine and additionally is susceptible to proteolytic degradation under N starvation. It was also found to assemble into nanotubes (He et al., 2009) and under advanced cellular starvation into inactive filaments (Petrovska et al., 2014). In *E. coli*, the activity of the Iß-type GS (EcGS) is controlled by cumulative feedback inhibition and covalent modification (reviewed in Reitzer, 2003). It has been shown that each of the 12 subunits can be modified by adenylylation (Tyr397) resulting in an inactivation of the respective subunit (Stadtman, 1990). Moreover, the adenlylylation of single subunits makes the other subunits more susceptible to cumulative feedback inhibition by various substances (Stadtman, 1990). These substances either bind the glutamine-binding pocket or have an allosteric binding site (Liaw et al., 1993; Woolfolk and Stadtman, 1967). The dodecameric structure of EcGS has been known for a long time (Almassy et al., 1986; Yamashita et al., 1989). However, when artificially exposed to divalent cations (Mn^{2+}, Co^{2+}) it randomly aggregates and produces long hexagonal tubes (paracrystalline aggregates) (Valentine et al., 1968). The detailed structural information on the mechanisms of this reversible GS-filament formation to an inactive form of EcGS, often associated with stress responses, has only recently been described by cryo-electron microscopy (cryo-EM) analysis (Huang et al., 2022). The *B. subtilis* GS has been shown to be feedback regulated. In addition, binding of the transcriptional repressor GlnR to the feedback inhibited complex not only activates the transcription repression function of GlnR (Fisher and Wray, 2008) but also stabilizes the inactive GS conformation potentially changing from a dodecamer into a tetradecameric structure (Travis et al., 2022a).

In *M. mazei,* a mesophilic methanoarchaeon, which is able to fix N_2, regulation of the central N metabolisms has been studied extensively on the transcriptional and post-transcriptional level (Jäger et al., 2009; Prasse and Schmitz, 2018; Veit et al., 2005). A central role of 2-OG for the perception of changes in N availabilities has been proposed, as has been demonstrated for cyanobacteria (Forchhammer, 1999; Herrero et al., 2001). The activity of *M. mazei* GS, encoded by $glnA_1$, is regulated by several different mechanisms. $GlnA_1$ is not covalently modified in response to N availability and thus represents a Iα-type-GS (Ehlers et al., 2005). It has been proposed, that $GlnA_1$ is directly activated under N starvation by the high intracellular concentrations of the metabolite 2-OG (Ehlers et al., 2005). 2-OG represents the internal signal for N limitation, since the internal 2-OG level significantly increases due to missing consumption by GDH under N starvation (*M. mazei* contains the oxidative TCA part, anabolic). The increased

cellular 2-OG concentration has been shown to be directly perceived by $GlnA_1$, most likely by direct binding resulting in strong activation (Ehlers et al., 2005). Besides, we showed first evidence that two small proteins interact with *M. mazei* $GlnA_1$, the PII-like protein $GlnK_1$ and small protein sP26 comprising 23 amino acids (Ehlers et al., 2005; Gutt et al., 2021). The presence and potential interaction of both small proteins showed small effects on the $GlnA_1$ activity. However, those small effects might be neglectable compared to the strong 2-OG stimulation, particularly taking into account that the indirect GS activity assay shows high deviations in the low activity range. Moreover, initial complex formation analysis by a pull-down approach indicated that in the absence of 2-OG the $GlnA_1$/$GlnK_1$ complexes are more stable than in the presence of high 2-OG. This led to the conclusion that due to the shift to N sufficiency after a period of N limitation, $GlnA_1$ activity is reduced due to the lower 2-OG concentration, but also due to a potential inhibitory protein interaction with $GlnK_1$ (Ehlers et al., 2005). Very recently, the first structural analysis of *M. mazei* $GlnA_1$ was reported, showing GS complexes with $GlnK_1$ (Schumacher et al. 2023). Based on their findings, Schumacher et al. propose a regulation of $GlnA_1$ activity by oligomeric modulation, with $GlnK_1$ stabilizing the dodecameric structure and the formation of $GlnA_1$ active sites. Since that work is entirely missing the effects of 2-OG on $GlnA_1$ structure and activity, we here aimed to study the regulation of *M. mazei* $GlnA_1$ in more detail by evaluating oligomerization and complex formation between $GlnA_1$, $GlnK_1$ and sP26 in dependence of 2-OG. This was achieved by employing mass photometry (MP), allowing molecular weight distribution of single complexes in solution, and by high resolution cryo-EM, whilst also performing activity assays.

Results

2-OG is responsible for $GlnA_1$-dodecamer formation in M. mazei

The strep-tagged purified $GlnA_1$ was analyzed by SEC in the presence of 12.5 mM 2-OG demonstrating that GS is exclusively present in a dodecameric structure, no other oligomers were detectable (suppl. Fig. S1). To investigate the effects of 2-OG on *M. mazei* $GlnA_1$ in more detail, we employed MP, a method that allows to measure the molecular weight distribution of particles in solution. Strep-tagged purified $GlnA_1$ (after SEC) was dialyzed into a 2-OG free HEPES buffer (see Materials and Methods) and subsequently analyzed by MP, demonstrating that in the presence of low 2-OG concentrations (0.1 mM) all of the *M. mazei* $GlnA_1$ was nearly exclusively present as dimers with no higher molecular weight complexes present. After addition of 12.5 mM 2-OG, the size distribution shifted towards a higher molecular weight complex of 630-700 kDa (calculated based on the measured dimer-size in each measurement; expected molecular weight of dodecamer: 634 kDa) (**Fig. 1A, B**). This molecular weight corresponds to a fully assembled dodecamer species, the same oligomeric structure that is adapted in GS from other prokaryotes. Using 2-OG concentrations varying between 0.1 and 12.5 mM, complex analysis showed that up to 62 % of all particles were assembled in a dodecamer. This allowed to determine the effective concentration of 2-OG for dodecamer assembly to be EC50 = 0.75 ± 0.01 mM 2-OG (based on two biological replicates, calculated with the percentage of dodecamer) as described in Materials and Methods, and further verified that no other intermediate oligomeric complexes were detectable during dodecameric assembly (**Fig. 1A, C**, suppl. Fig. S2A, B). Notably, $GlnA_1$ did not reach 100 % dodecamer-assembly after removal and re-addition of 2-OG, although only dodecameric $GlnA_1$ was used for dialysis (suppl. Fig. S1B, C). We conclude that $GlnA_1$ is rather unstable in the absence of 2-OG and some of the protein loses its ability to oligomerize after 2-OG was removed by dialysis.

Furthermore, 2-OG did not only cause dodecamer-assembly but also higher enzyme activity. Activity measurements of Strep-$GlnA_1$ in the presence of increasing 2-OG concentrations showed a strong increase from 0.0 U/mg in the absence of 2-OG up to 7.8 ± 1.7 U/mg in the presence of 12.5 mM 2-OG (six independent protein purifications). The EC50 for $GlnA_1$ activity was determined to be 6.3 mM 2-OG (**Fig. 1D**). Thus, we conclude that 2-OG first acts as a trigger for dodecameric

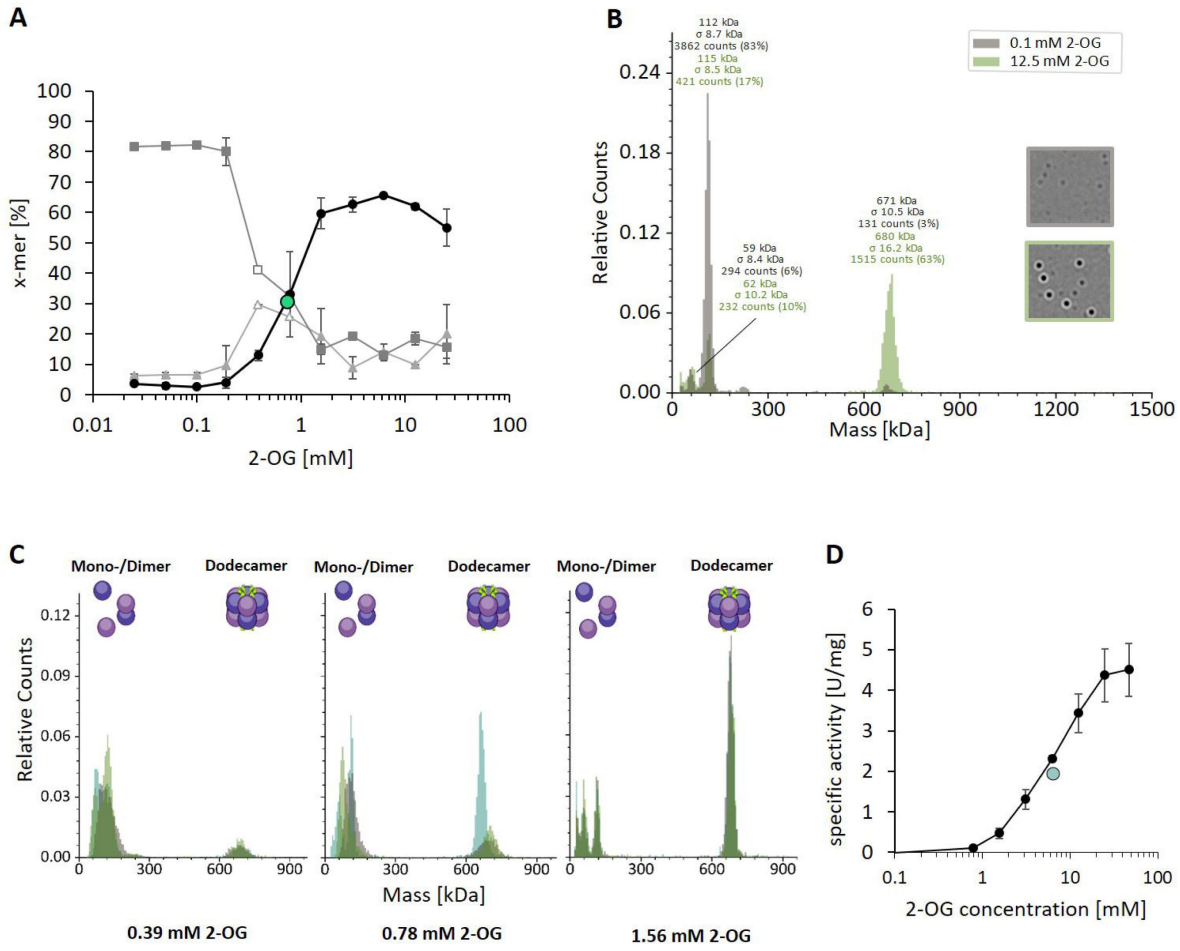

Figure 1

$GlnA_1$-dodecamer-assembly is induced by 2-OG without detectable oligomeric intermediates.

Oligomerisation states of purified strep-tagged $GlnA_1$ were assessed in dependence of 2-OG by mass photometry as described in MM using a Refeyn TwoMP mass photometer (Refeyn Ltd., Oxford, UK). Mass spectra are shown with relative counts (number of counts per peak in relation to the total number of counts) plotted against the molecular weight. **A**: 75 nM $GlnA_1$ were preincubated in the presence of varying 2-OG concentrations (0 to 25 mM) for ten min at room temperature and kept on ice until measurement. The percentage of monomer (▲), dimer (■) and dodecamer (●) considering the total number of counts was plotted against the 2-OG concentration. One out of two independent biological replicates with each three technical replicates is shown exemplarily and the EC50 for dodecamer-assembly is indicated in green. Monomer and dimer-peaks were difficult to distinguish in the measurements for 0.39 and 0.78 mM 2-OG and the values are therefore shown without standard deviation and in white. **B**: Exemplary mass spectra of $GlnA_1$ oligomers in the presence of 0.1 and 12.5 mM 2-OG. The molecular masses shown above the peaks correspond to a Gaussian fit of the respective peak (Gaussian fit not shown). **C**: Mass spectra of the three technical replicates (different green colors) of $GlnA_1$-oligomers at 0.39, 0.78 and 1.56 mM 2-OG, excluding the presence of intermediates. **D**: The specific activity of purified strep-tagged $GlnA_1$ was determined as described in MM in the presence of varying 2-OG concentrations (0, 0.78, 1.56, 3.13, 6.25, 12.5, 25 and 47 mM). The EC50 for $GlnA_1$-activity is shown in green and the standard deviation of four technical replicates is depicted.

assembly of *M. mazei* $GlnA_1$ (with an EC50 = 0.75 mM 2-OG), setting it apart from other bacterial and eukaryotic enzyme variants. Moreover, most likely in addition to the dodecameric assembly, 2-OG is required for a further 2-OG induced conformational switch of the active site, since saturated $GlnA_1$ activities are not reached in the presence of 5 mM 2-OG, when most of the $GlnA_1$ is in a dodecameric structure. For full activity, the presence of at least 12.5 mM 2-OG is required (EC50 = 6.3 mM 2-OG).

$GlnK_1$ has no detectable effects on GS dodecamer assembly or activity under the tested conditions

Previous studies have shown protein interactions between *M. mazei* $GlnA_1$ and $GlnK_1$ as well as $GlnK_1$ induced effects on $GlnA_1$ activity (ratio $GlnA_1$:$GlnK_1$ 1:1, (Ehlers et al. 2005) and 2:1.4 (Gutt et al., 2021) in activity assays). Consequently, we next tested the effects of $GlnK_1$ on $GlnA_1$ oligomerization in the presence of 2-OG. Performing the MP analysis under the tested conditions as before but in the presence of purified $GlnK_1$, demonstrated that (i) in the absence of 2-OG varying ratios between $GlnA_1$ and $GlnK_1$ (20:1, 2:1, 2:10 calculated based on monomer mass) did not result in any dodecamer assembly of $GlnA_1$ (**Fig. 2A, B**), (ii) no difference in the $GlnA_1$ dodecameric assembly in the presence of 2-OG was obtained in the presence of purified $GlnK_1$ (ratio 2:1), (iii) nor was binding of $GlnK_1$ to $GlnA_1$ detected by a respective increase in the mass of the higher oligomeric complex (**Fig. 2B, C**). Moreover, the presence of $GlnK_1$ (ratio 2:1) neither had an influence on the 2-OG affinity (EC50 (- $GlnK_1$) = 1.06 mM 2-OG; EC50 (+ $GlnK_1$) = 1.02 mM 2-OG, EC50 calculated based on the dodecamer/dimer ratio), nor in any ratio on the specific activity of $GlnA_1$ (**Fig. 2 D, E**: exemplarily showing 2:1; suppl. Fig. S2C, D). Consequently, we conclude that under the conditions tested using purified proteins, $GlnA_1$ dodecamer assembly occurs independently of $GlnK_1$ and no binding of $GlnK_1$ to the dodecameric $GlnA_1$ occurs. However, we cannot exclude that cellular components/metabolites not present in these experiments are crucial for a $GlnA_1$-$GlnK_1$ interaction.

Structural basis of oligomer formation by 2-OG

To now unravel the structural mechanism underlying *M. mazei* $GlnA_1$ activation by 2-OG, we employed cryo-EM and single-particle analysis. Treating freshly purified Strep-$GlnA_1$ with 12.5 mM 2-OG, effectively shifted the equilibrium towards fully assembled homo-oligomers as depicted in the MP experiments (suppl. Fig. S1C). In the micrographs, fully assembled ring-shaped particles are visible. However, initial attempts to obtain a 3D reconstruction were hindered by the pronounced preferred orientation of particles within the ice, a challenge which has been overcome by introducing low concentrations of CHAPSO (0.7 mM). In our final dataset, all particles exhibited well-distributed oligomers in diverse orientations. Leveraging this dataset, we aligned the particles to a 2.39 Å resolution structure, revealing well resolved side chains that facilitated seamless model building (**Fig. 3**, suppl. Fig. S3, suppl. Tab. S2). Consequently, we achieved a structure demonstrating excellent geometry and density fitting.

The detailed structural analysis uncovered that $GlnA_1$ assembles into a dodecamer characterized by stacked hexamer rings. A single $GlnA_1$ protomer is composed of 15 β-strands and 15 α-helices and is split in into a larger C-domain and an N-domain by helix α3. The dodecameric arrangement is achieved through two distinct interfaces, the hexamer interfaces and inter-hexamer interfaces. Hexamer interfaces are situated between subunits within each ring, while inter-hexamer interfaces occur between subunits derived from adjacent rings (**Fig. 4A, B, C**). The structures are highly similar to Gram-positive bacterial GS structures (PDB: 4lnn, Murray et al., 2013), with root mean squared deviations (rmsds) of 0.5–1.0 Å.

A closer inspection of the density reveals the density for the bound 2-OG at an allosteric site localized at the interface between two $GlnA_1$ protomers in vicinity of the $GlnA_1$ catalytic site (**Fig. 4B, D**). Several residues are contributing to its binding. R172’ and S189’ coordinate the γ-

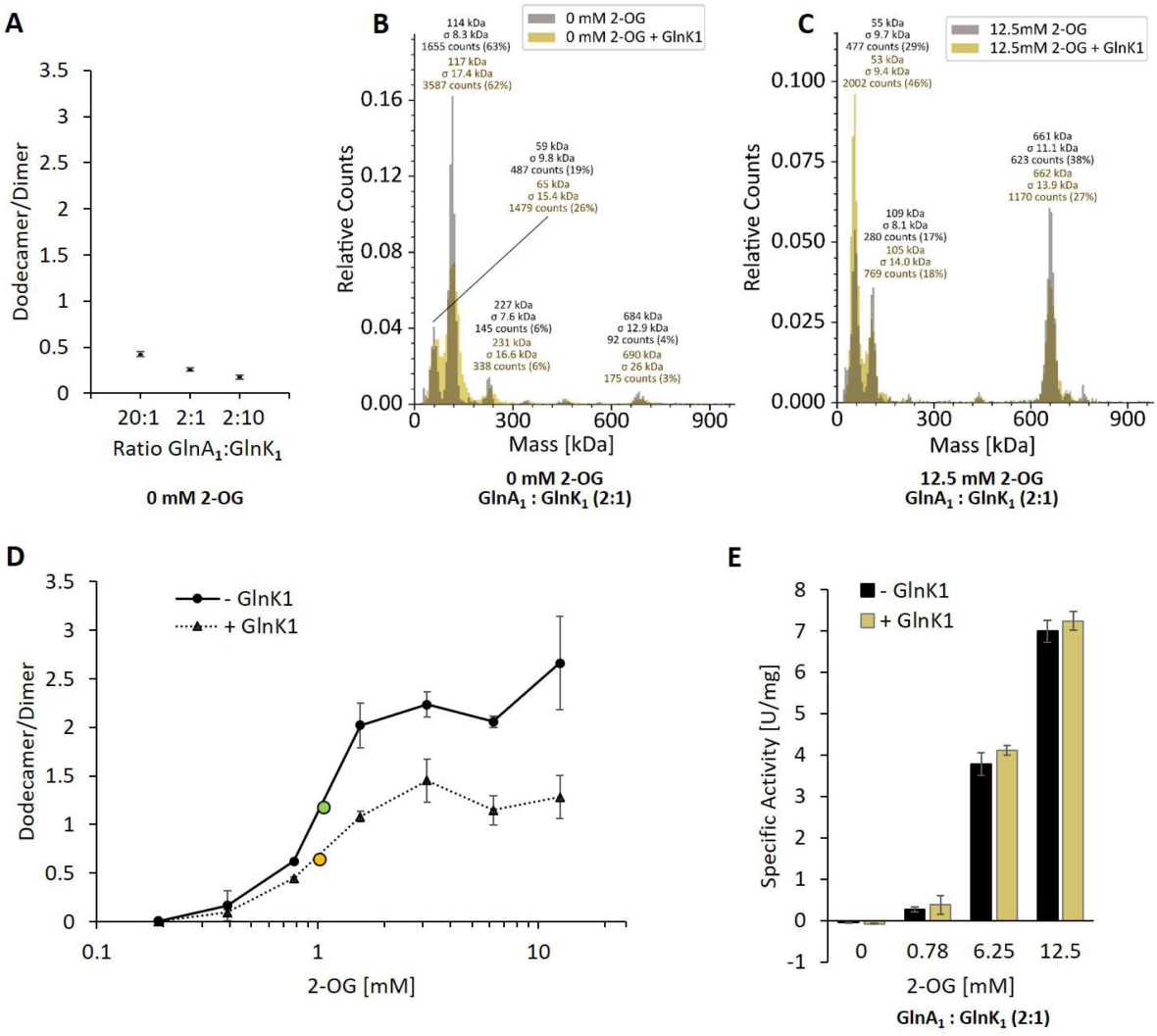

Figure 2

$GlnA_1$-dodecamer-assembly and activity are not influenced by $GlnK_1$ under the conditions tested.

Purified strep-tagged $GlnA_1$ and tag-less $GlnK_1$ were incubated in the absence or presence of 2-OG in varying concentrations for ten min at RT. Oligomerisation states were assessed by mass photometry. Mass spectra are shown with relative counts (see **Fig. 1**). **A**: The obtained ratio of $GlnA_1$ dodecamer/dimer of three technical replicates are shown for varying ratios between $GlnA_1$ and $GlnK_1$ (20:1, 2:1, 2:10, ratios relating to monomers) in the absence of 2-OG. **B, C**: Exemplary mass spectra of $GlnA_1$ incubated in the absence and presence of $GlnK_1$ (2:1) at 2-OG concentrations of 0 mM (B) and 12.5 mM (C). The molecular masses shown above the peaks correspond to a Gaussian fit of the respective peak (Gaussian fit not shown). **D**: 200 nM $GlnA_1$ (molarity calculated based on molecular mass of monomers) were preincubated with $GlnK_1$ (in a 2:1 ratio) in the presence of varying 2-OG concentrations (0.19 to 12.5 mM) for ten min at RT. One biological replicate with three technical replicates was performed. The ratio of $GlnA_1$ dodecamer/dimer was plotted against the 2-OG concentration and the EC50 is indicated in green (●, - $GlnK_1$) and yellow (●, + $GlnK_1$). **E**: The specific activity of purified strep-tagged $GlnA_1$ in the absence and presence of $GlnK_1$ (ratio 2:1) was determined as described in MM in the presence of varying 2-OG concentrations (0, 0.78, 6.25 and 12.5 mM). The standard deviations of four technical replicates of one biological replicate are indicated.

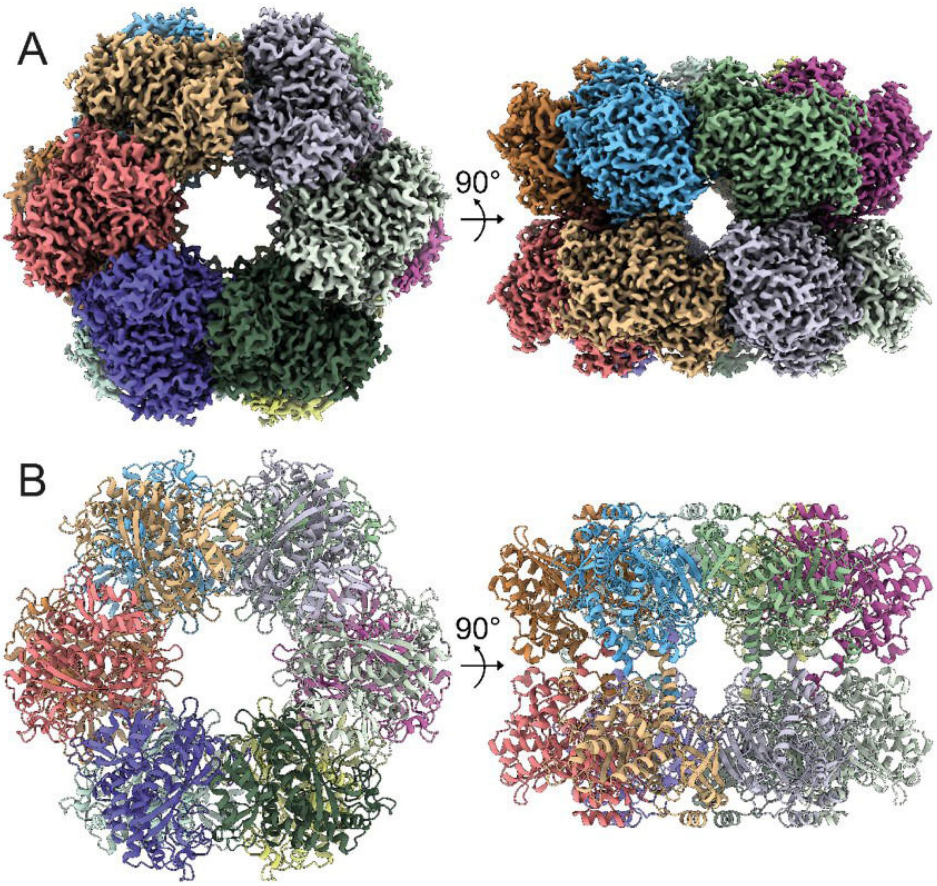

Figure 3

Structure of *M. Mazei* $GlnA_1$ with 2-OG.

A: Three-dimensional segmented cryo-EM density of the dodecameric complex colored by subunits. **B**: Corresponding views of the $GlnA_1$ atomic model in cartoon representation.

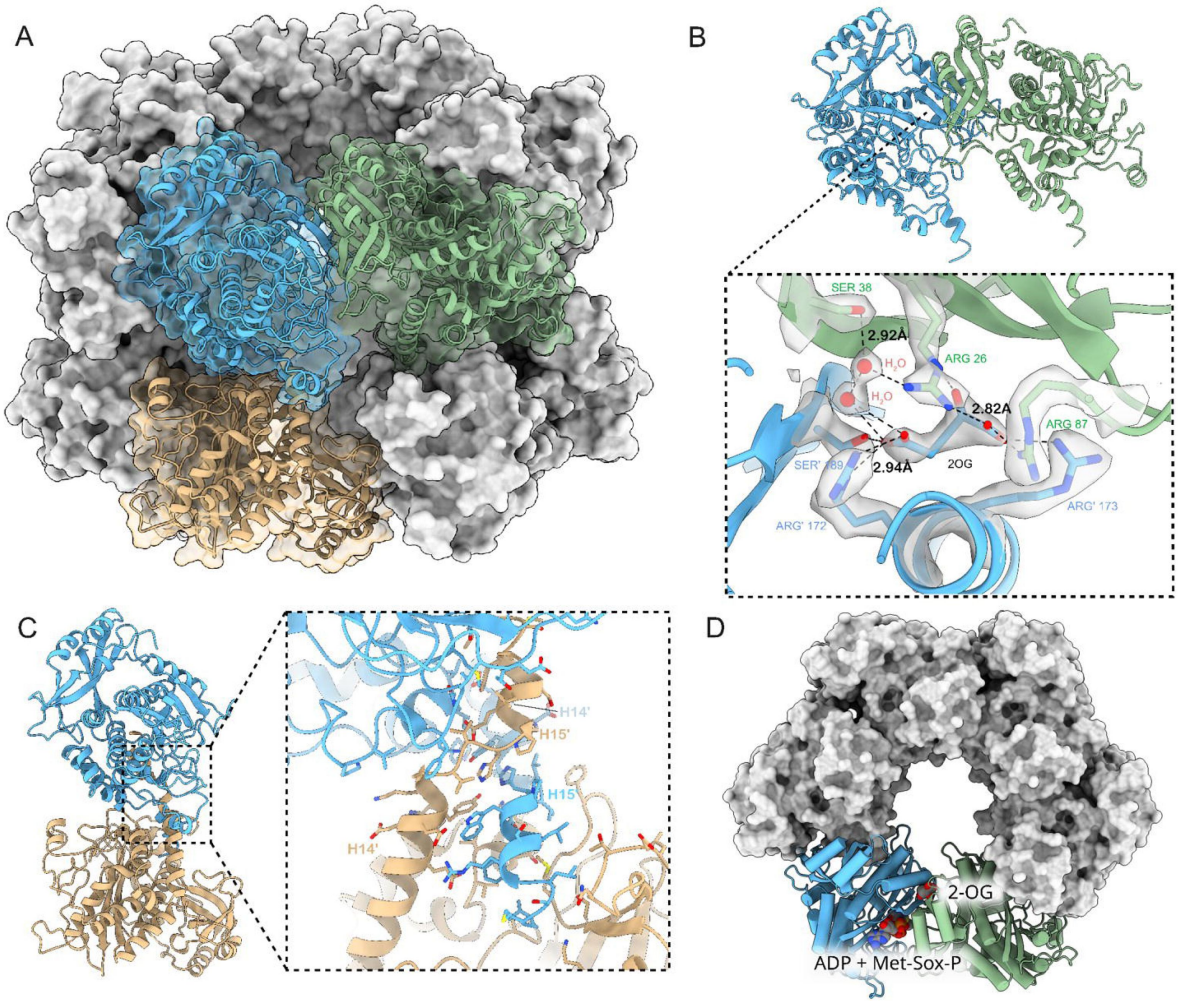

Figure 4

Hexameric interface, inter-hexameric interface and 2-OG binding site of dodecameric $GlnA_1$.

A: Surface representation of the *M. mazei* $GlnA_1$ 2-OG dodecamer with three $GlnA_1$ protomers fitted in cartoon representation into the dodecamer as dimers of inter-hexameric (blue and ochre) and hexameric (blue and green) $GlnA_1$. **B**: Horizontal dimers and close-up of 2-OG binding site. Important residues are shown as atomic stick representation, primed labels indicate neighboring protomer. 2-OG and water molecules important for ligand binding fitted into density are shown in grey. Dotted lines represent polar interactions between 2-OG, waters and residues. **C** Vertical dimers and close-up of dimerization site. C-terminal helices H14/15 and H14'/ H15' of two neighboring protomers lead to tight interaction, mediated by hydrophobic and polar interactions. **D**: Top-view of $GlnA_1$ hexamer, 2-OG and substrate binding sites are depicted for one horizontal dimer.

Carboxy-group. Additionally, two tightly bound water molecules are detectable in the binding site. One is interacting with the γ-Carboxy group, while being stabilized by another water that is coordinated by S38 and R26. Latter arginine is coordinating the α-Keto-group and, together with R87 and R173', the α-Carboxy group of 2-OG (**Fig. 4B**). Notably, F24 stabilizes the 2-OG via stacking with its phenyl ring (**Fig. 5**). This binding contribution from two $GlnA_1$ protomers at the intersubunit junction enhances activation by boosting readiness and the rate of full complex assembly. It operates akin to molecular glue that facilitate the observed cooperative assembly.

A comparison with the substrate-bound $GlnA_1$ structure (PDB: 8tfk, Schumacher et al. 2023) revealed that the catalytically important residues in *M. mazei* are the aspartic acid (D57), that abstracts the proton from ammonium, and the catalytic glutamic acid, Glu307. The active site of *M. mazei* $GlnA_1$ is formed at the interface between two subunits in the hexamer and formed by five key catalytic elements surrounding the active site: the E flap (residues 303–310), the Y loop (residues 369–377), the N loop (residues 235–247), the Y* loop (residues 152–161) and the D50' loop (residues 56-71). The latter one is the only one that originates from adjacent neighboring protomer (**Fig. 5C, E**).

Superposition of our structure with the apo- *M. mazei* structure (PDB: 8tfb, Schumacher et al., 2023) reveals that 2-OG binding also triggers further movements that lead to structural changes in the substrate binding pocket (**Fig. 5A, B, D**). R87' and its loop undergo a dramatic flip to coordinate 2-OG and D170 of helix α3 (residues 167-181) (**Fig. 5A**). This, combined with the action of other coordinating residues, initiates a motion that is propagated through the entire protein. Notably, helix α3 shifts forward, causing F184 to flip over and facilitate a T-shaped aromatic interaction with F202. The resulting pull on F202 causes F204 to flip, allowing π-stacking with the purine moiety of ATP (**Fig. 5B**). This series of structural changes primes the active site for ATP binding by already adopting the side chain conformations that are observed in analogue (Met-Sox-P-ADP)-bound structure (transition state) (PDB: 8tfk, Schumacher et al., 2023), thus facilitating nucleotide binding (**Fig. 5C, E**).

Additionally, the D50' loop adopts a position similar to the transition state in a catalytic competent conformation. This involved a remodeling of the loop, leading to the positioning of key catalytic residues in a catalytic competent configuration. Compared to the apo structure (Schumacher et al., 2023), R66 flips out of the catalytic pocket, now accommodating R319 which participates in phosphoryl transfer catalysis (Liaw and Eisenberg, 1994) (**Fig. 5D**). In addition, Asp 57' moves deeper into the binding site, facilitating the proton abstraction of NH_4^+ and preparing for its attack on the phosphorylated glutamate. Similar to the ATP/ADP binding site, these catalytic elements are primed to ideally stabilize the tetrahedral open active state. This is illustrated by the superposition of the inhibitor-bound, transition-state locked structure (Schumacher et al., 2023) (**Fig. 5C, E**).

Feedback inhibition by glutamine does not affect the dodecameric M. mazei $GlnA_1$ structure

For bacteria it is known, that GS can be feedback inhibited. Very recently, the first feedback inhibition of an archaeal GS by glutamine has been reported for *Methermicoccus shengliensis* GS (Müller et al., 2024). The specific arginine residue identified to be relevant for the feedback inhibition is R66. Consequently, we generated the respective *M. mazei* $GlnA_1$ mutant protein changing the conserved arginine to alanine (R66A) (see also **Fig. 5D, E**) and compared the purified strep-tagged mutant protein with the wildtype (wt) protein. In the presence of 12.5 mM 2-OG, the mutant protein showed the same specific activity as obtained for the wt. However, when supplementing 5 mM glutamine, exclusively the wt was strongly feedback inhibited, whereas the R66A mutant protein was not significantly affected (**Fig. 6A**). In *B. subtilis*, R62 is responsible for feedback inhibition. The superposition of the apo-BsGS structure (PDB: 4lnn, Murray et al., 2013) with our 2-OG-bound $GlnA_1$ reveals a similar positioning of the respective *M. mazei* R66 (**Fig. 6B**) indicating a similar mechanism. Moreover, we can rule out an effect on the oligomeric

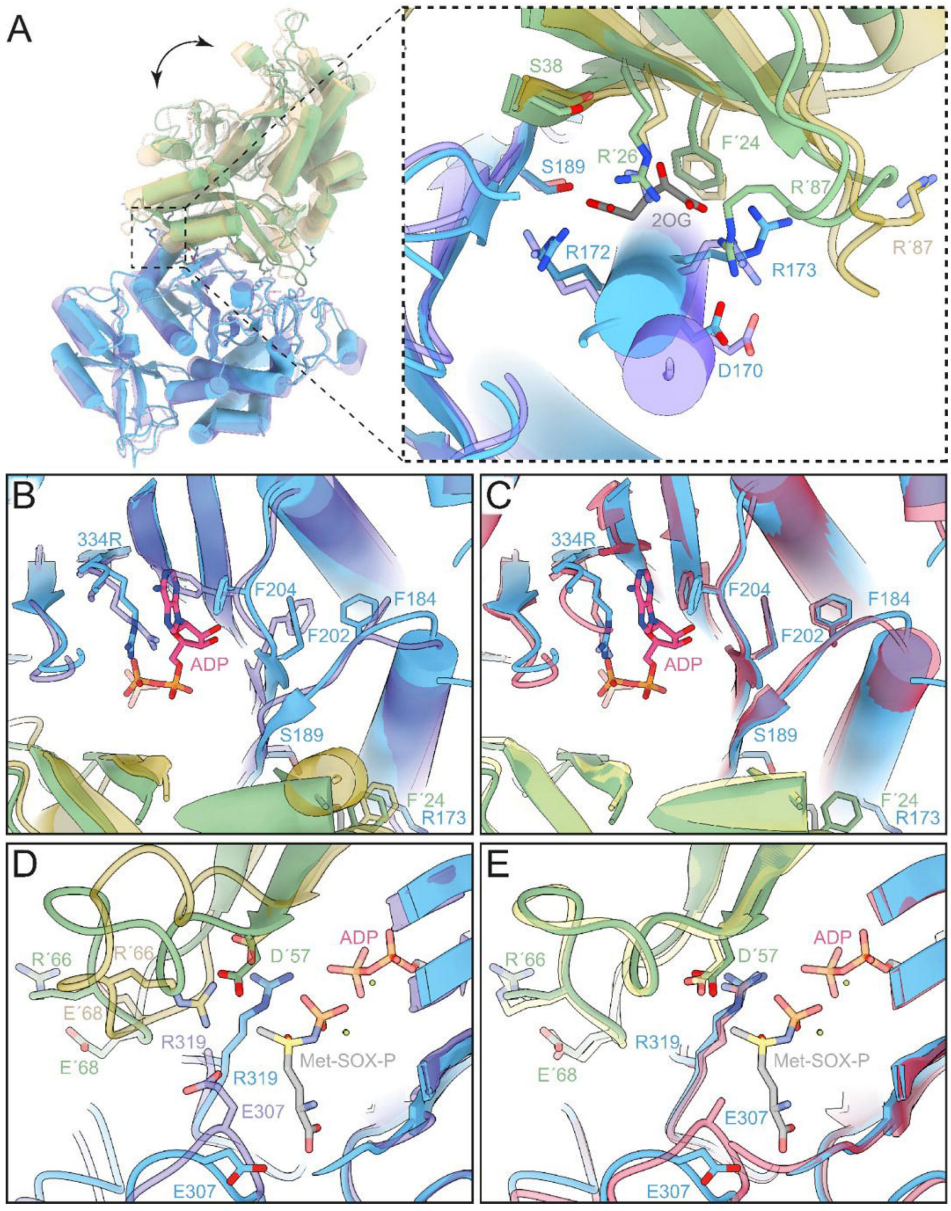

Figure 5

Comparison of 2-OG and substrate binding site of 2-OG bound, apo and TS structures

(Schumacher et al., 2023). Atomic models in cartoon, important residues shown in stick representation. Colors: *M. mazei* $GlnA_1$ 2-OG - blue/green, *M. mazei* $GlnA_1$ apo (PDB: 8tfb, Schumacher et al., 2023) - purple/ochre and *M. mazei* $GlnA_1$ Met-Sox-P·ADP (PDB: 8tfk, Schumacher et al., 2023) transition state ($GlnA_1$ TS) - red/yellow. **A** *left:* $GlnA_1$ 2-OG dimer in superposition with $GlnA_1$ apo showing large scale movements upon 2-OG binding. **A** *right:* Close-up of 2-OG binding site of $GlnA_1$ 2-OG in superposition with $GlnA_1$ apo. Dramatic movement of Helix α3 (residue 167-181) and R87 loop show effect of 2-OG binding. **B**: Close-up of substrate binding site of $GlnA_1$ 2-OG in superposition with $GlnA_1$ apo and ADP ligand from $GlnA_1$ TS. Helix α3 movement upon 2-OG binding leads to a cascade of conformational changes of the phenylalanines F184, F202 and F204 that lead to a priming of the active site for ATP binding. **C**: Close-up of substrate binding site of $GlnA_1$ 2-OG in superposition with $GlnA_1$ TS shows high similarity between 2-OG bound and transition state structure. **D**: Close-up of substrate binding site of $GlnA_1$ 2-OG in superposition with $GlnA_1$ apo and Met-Sox-P ligand from $GlnA_1$ TS. Large structural changes of the D50-loop with ejection of the R66 key-residue shown. Flipping of the loop allows R319 and D57 to move in further and catalyze phosphoryl-transfer and attack of NH_4^+, respectively. **E**: Close-up of the substrate binding site of $GlnA_1$ 2-OG in in superposition with $GlnA_1$ TS reveals strong similarity between 2-OG bound and transition state structure in the active site.

structure of $GlnA_1$ by MP analysis, clearly showing that glutamine does not induce disassembly of the dodecameric wt $GlnA_1$ (**Fig. 6C**). Instead, this effect can be explained with the role of R66 being an important residue to bind to glutamine in the product state of the enzyme.

Discussion

2-OG is crucially required for M. mazei GS assembly to an active dodecamer and induces the conformational shift towards an active open state

In *M. mazei*, increased 2-OG concentrations act as central N starvation signal (Ehlers et al., 2005). Here, we demonstrated the importance of 2-OG as the major regulator of *M. mazei* $GlnA_1$ activity by using independent methods, MP and cryo-EM, to detect and structurally characterize single complexes with high resolution and quantify different oligomeric states of $GlnA_1$. We have found mainly dimeric $GlnA_1$ (apo $GlnA_1$) to be inactive and crucially require 2-OG to form an active dodecameric complex. Moreover, this dodecameric conformation is the only active state of $GlnA_1$. In the first step, 2-OG assembles the dodecamer by binding at the interface of two subunits (**Fig. 4B**) and functions as a molecular glue between neighbouring subunits. The assembly upon 2-OG addition observed using MP appears to be cooperative, fast and without any detectable intermediate states (**Fig. 1B, C**). Only immediately after thawing a frozen purified $GlnA_1$ preparation and in case that no additional SEC was performed prior to MP analysis, samples showed additional octameric complexes in MP with low abundancy (suppl. Fig. S4). However, octameric complexes were never observed in cryo-EM or detected by SEC analysis of frozen purified $GlnA_1$ samples. Consequently, octamers are most likely broken or disassembled $GlnA_1$-dodecamers or dead-ends in assembly with no physiological function, rather than an incomplete dodecamer during assembly. Thus, our findings are contrary to the assembly model proposed by Schumacher et al. (Schumacher et al., 2023).

As a second step of activation, the allosteric binding of 2-OG causes a series of conformational changes in $GlnA_1$ protomers, which prime the active site for the transition state and hence catalysis of the enzyme. This conformational change of the ATP-binding pocket of the dodecameric $GlnA_1$ upon 2-OG binding goes hand in hand with the observed increased activity at higher 2-OG concentrations (**Fig. 1**). Comparing our 2-OG-bound $GlnA_1$ dodecameric structure and the dodecameric *M. mazei* $GlnA_1$ transition state (PDB: 8tfk) and apo structures (PDB: 8ftb) reported by Schumacher et al. (Schumacher et al., 2023), clearly demonstrates that 2-OG transfers $GlnA_1$ into its open active state conformation (**Fig. 5**). The conformation of our 2-OG-bound dodecamer resembled the transition state conformation (ADP-Met-Sox-bound complex) reported by Schumacher et al., even though in our case no ATP was added (**Fig. 5E**). A reconfiguration of the active site upon 2-OG-binding has also been reported for GS in *Methanothermococcus thermolithotrophicus* (Müller et al., 2024). In this report, which does not delineate dodecamer assembly at all, it was demonstrated that binding of 2-OG in one protomer-protomer interface of a dodecameric GS causes a cooperative domino effect in the hexameric ring of *M. thermolithotrophicus* GS (Müller et al., 2024). A 2-OG bound protomer undergoes a conformational change and thereby induces the same shift in its neighbouring protomer (Müller et al., 2024). This is comparable to our observed cooperativity of *M. mazei* dodecamer assembly at low 2-OG concentrations (EC50 = 0.75 mM, calculated based on the percentage of dodecamer). On the other hand, *M. mazei* $GlnA_1$ reaches maximal activity only at much higher 2-OG concentrations (EC50 = 6.3 mM 2-OG) and likely requires a fully 2-OG-occupied dodecamer for maximal activity. The difference between the two EC50 values strongly points towards the dodecamer-assembly being induced by only one 2-OG per hexameric ring, whilst the maximum activity requires one 2-OG in every 2-OG binding site (in agreement with roughly 6-fold higher EC50). The here obtained high activities by 2-OG saturation (up to 9 U/mg), in comparison with previously described *M.*

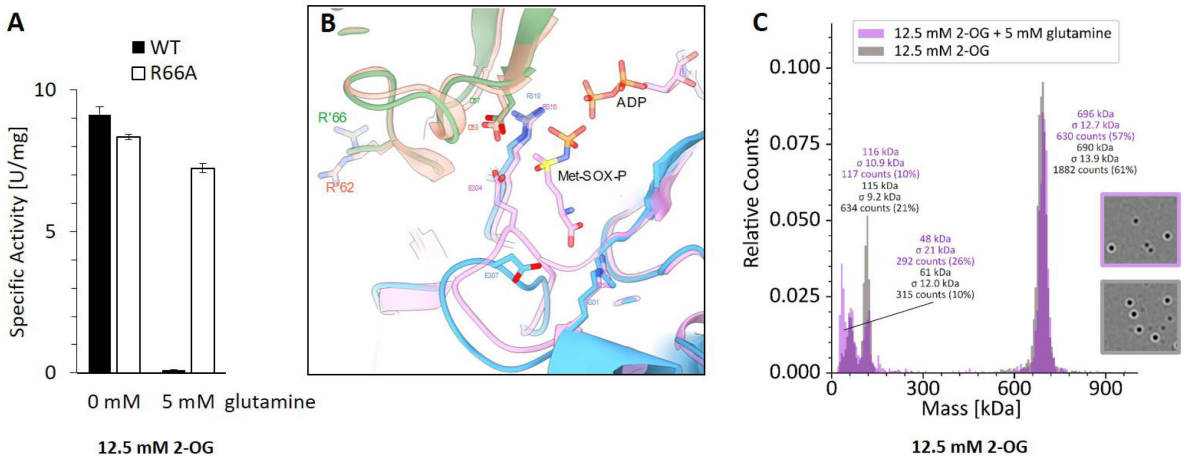

Figure 6

Feedback inhibition of $GlnA_1$ by glutamine.

A: Specific activity of purified strep-tagged $GlnA_1$ (wt) and the respective R66A-mutant protein was determined as described in Materials and Methods in the presence of 12.5 mM 2-OG and after additional supplementation of 5 mM glutamine. For wt and the R66A-mutant one out of two biological independent replicates are exemplarily shown, the deviation indicates the average of four technical replicates. **B:** Superposition GS structures without glutamine of *M. mazei* (blue, green) and *B. subtilis* (orange, pink; PDB: 4lnn, Murray et al., 2013): substrate binding-site including R'66 (R'62, respectively), which are responsible for feedback inhibition. **C**: Exemplary mass spectra of Strep-$GlnA_1$ with 12.5 mM 2-OG in presence and absence of 5 mM glutamine. The molecular masses shown above the peaks correspond to a Gaussian fit of the respective peak (Gaussian fit not shown).

mazei $GlnA_1$ activities in the absence of 2-OG in a significantly lower range (mU/mg) (Gutt et al., 2021; Schumacher et al., 2023), support our conclusion that 2-OG is substantial for the $GlnA_1$ active state.

$GlnA_1$ activity is further regulated by feedback inhibition, small proteins and possibly filament formation

M. mazei $GlnA_1$ belongs to the group of Iα-type GS, which are known to be feedback inhibited. We confirmed a strong feedback inhibition by a genetic approach and validated R66 to be the key residue for this inhibition (**Fig. 6**) as suggested in Müller et al. 2024. The mechanism of feedback inhibition has been described in detail for *B. subtilis* GS (Murray et al., 2013). There, R62 plays the central role by binding glutamine and inducing a well ordered inactive structure at the substrate-binding pocket upon glutamine-binding (Murray et al., 2013). The homologous *M. mazei* R66 likely conveys a similar way of inhibition to *B. subtilis* GS (**Fig. 6B**, alignment in suppl. Fig. S5).

Further regulations by the two small proteins sP26 and the PII-like protein $GlnK_1$ have previously been reported for *M. mazei* (Ehlers et al., 2005; Gutt et al., 2021; Schumacher et al., 2023). Moreover, in previous reports, $GlnK_1$ was shown to interact with $GlnA_1$ in vivo after a nitrogen upshift by pull-down approaches (Ehlers et al., 2005), pointing towards an inhibitory function of $GlnK_1$ under shifting conditions from N limitation to N sufficiency. However, in the present study, neither an interaction with $GlnK_1$, nor $GlnK_1$ effects on $GlnA_1$ complex formation analysed by MP, nor an effect of $GlnK_1$ on $GlnA_1$ activity was detectable under the conditions used at varying 2-OG concentrations (0.1 to 12.5 mM) and ratios of $GlnK_1$ to $GlnA_1$ (20:1, 2:1, 2:10) (**Fig. 2**). Moreover, the addition of $GlnK_1$ did not result in a change of the EC50 of 2-OG for the dodecamer $GlnA_1$ assembly (**Fig. 2D**). Similarly, we could not determine a cryo-EM structure including sP26 despite adding large excess of the small protein either obtained by co-expression or by addition of a synthetic peptide. Because these attempts were unsuccessful, we speculate that yet unknown cellular factor(s) might be required for an interaction of $GlnA_1$ with both small proteins, $GlnK_1$ and sP26, which however is difficult to simulate under in vitro conditions with purified proteins. Taken this into account, we speculate about a potential function of the two small proteins beyond $GlnA_1$ inactivation or activation. Since the $GlnA_1$ reaction is coupled to the GOGAT reaction (GS/GOGAT system) and the products of the two reactions replenish the substrates for one other, it is tempting to speculate that $GlnA_1$ and GOGAT experience metabolic coupling by sP26 and/or $GlnK_1$, e.g. by being involved in recruiting or separating GOGAT from $GlnA_1$.

Finally, higher oligomeric states of GS enzymes have been known for a long time for organisms like yeast and *E. coli* (He et al., 2009; Huang et al., 2022; Petrovska et al., 2014; Valentine et al., 1968). Interestingly, dependent on the ice thickness and on higher concentrated areas of the grids, we could also observe filament-like structures of *M. mazei* $GlnA_1$ in cryo-EM and resolved their structure at a resolution of 6.9 Å (suppl. Fig. S6). Such $GlnA_1$ filaments are also detectable in the cryo-EM images of Schumacher et al. 2023, but were not reported. The filament interface is much alike the previously reported *E. coli* GS filament structures (Huang et al., 2022). The physiological relevance of filamentation in *M. mazei* however remains unresolved and raises the question, whether an additional rapid modulation of $GlnA_1$ activity through higher oligomeric states exists. In yeast for example, GS filamentation was described as mostly depending on stress conditions (Petrovska et al., 2014).

M. mazei *$GlnA_1$ shows unique properties*

Overall, we have confirmed 2-OG to be the central activator of $GlnA_1$ in *M. mazei*, which assembles the active dodecamer and induces a conformational switch towards an active open state. Though 2-OG has previously been reported as an on-switch for (methano)archaeal GS activity (Ehlers et al., 2005; Müller et al., 2024; Pedro-Roig et al., 2013), the 2-OG-triggered dodecameric assembly

is novel and described exclusively for *M. mazei* $GlnA_1$. Neither in cyanobacteria, enterobacteria or *Bacillus* has 2-OG been reported as the sole direct activator of the enzyme, nor is complex (dis-)assembly a mode of regulating GS activity in any other of these model organisms. This is further supported by the absence of up to three of those four arginines which are coordinating 2-OG in *M. mazei* $GlnA_1$, in these organisms (suppl. Fig. S5). The cyanobacterial, enterobacterial and gram positive GS are assumed to be present in the cell as active dodecamers (Almassy et al., 1986; Bolay et al., 2018; Deuel et al., 1970). These dodecamers are inactivated upon sudden N sufficiency through very different mechanisms all including additional proteins (see **Fig. 7**). In *Synechocystis,* GS is blocked by small proteins, which are repressed under nitrogen limitation, one in a 2-OG-NtcA mediated way and the other one via a glutamine sensing riboswitch (Bolay et al., 2018; Klähn et al., 2018, 2015). The enterobacterial GS experiences 2-OG-PII dependent gradual adenylylation of subunits, which abolishes the enzyme activity, and *B. subtilis* GS is feedback inhibited by glutamine and further inhibited by binding of the transcription factor GlnR (Almassy et al., 1986; Stadtman, 2001; Travis et al., 2022b). Consequently, the GS regulation in *M. mazei* by a 2-OG triggered assembly is unique across all prokaryotic GS studied so far.

The direct 2-OG activation and glutamine feedback inhibition of *M. mazei* GS are two fast, reversible and very direct ways of reacting towards the changing N status of the cell. We propose that the direct activation through 2-OG without any required additional protein, as it is the case for all other regulations, is a more simple and direct regulation of GS. Due to the evolutionary placement of methanoarchaea and haloarchaea, where a direct 2-OG regulation has been found exclusively, this may represent an ancient regulation.

Materials and methods

Strains and plasmids

For heterologous expression and purification of Strep-tagged $GlnA_1$ (MM_0964), the plasmid pRS1841 was constructed. The $glnA_1$-sequence along with the sP26-sequence (including start-codon: ATG) were codon-optimized for *Escherichia coli* expression and commercially synthesized by Eurofins Genomics on the same plasmid (pRS1728) (Ebersberg, Germany). Polymerase chain reaction (PCR) was performed using pRS1728 as template and the primers (Eurofins Genomics, Ebersberg, Germany) GlnAopt_NdeI_for (5'TTTCATATGGTTCAGATGAAAAAATG3') and GlnA1opt_BamHI_rev (5'TTTGGATCCTTACAGCATGCTCAGATAACGG3'). The resulting $GlnA_1$_opt PCR-product and vector pRS375 were restricted with NdeI and BamHI (NEB, Schwalbach, Germany); the resulting pRS375 vector fragment and the $GlnA_1$ fragment were ligated resulting in pRS1841. For heterologous expression of Strep-$GlnA_1$, pRS1841 was transformed in *E. coli* BL21 (DE3) cells (Thermo Fisher Scientific, Waltham, Massachusetts) following the method of Inoue (Inoue et al., 1990). For generating the Arg66Ala-mutant, a site-directed mutagenesis was performed. pRS1841 was PCR-amplified using primers sdm_GlnA_R66A_for (5'ATTGAAGAAAGCGATATGAAACTGGCGC3') and sdm_GlnA_R66A_rev (5'**CGC**GGTAAAGCCCTGAATGCTGCTACC3') by Phusion High-Fidelity polymerase (Thermo Fisher Scientific, Waltham, Massachusetts) followed by religation resulting in plasmid pRS1951. For heterologous expression, pRS1951 was transformed into *E. coli* BL21 (DE3).

In order to co-express sP26 along with Strep-$GlnA_1$, the construct pRS1863 was generated. pRS1728 with the codon-optimized sP26-sequence and pET21a (Novagen, Darmstadt, Germany) were restricted with NdeI and NotI and the resulting untagged sP26_opt was ligated into the pET21a backbone yielding pRS1863. pRS1863 was co-transformed with pRS1841 into *E. coli* BL21 (DE3) cells (Thermo Fisher Scientific, Waltham, Massachusetts) selecting for both Kanamycin (pRS1841 derived) and Ampicillin (pRS1863 derived) resistance.

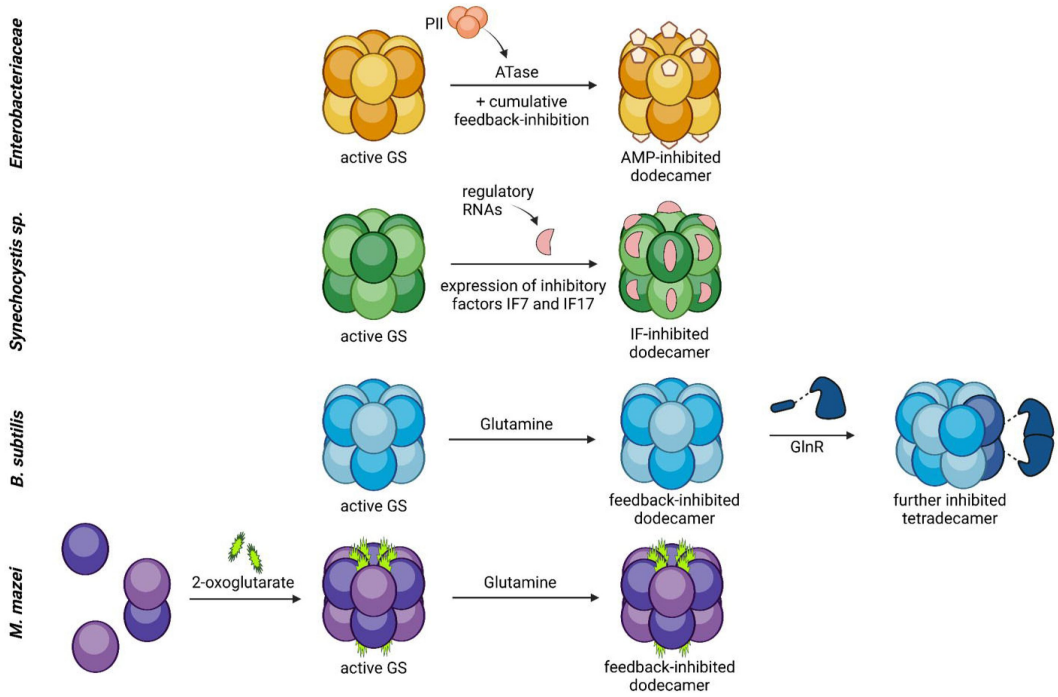

Figure 7

Model of the various molecular mechanisms of glutamine synthetase activity regulation.

Comparison of the regulation of glutamine synthetase activity in *E. coli /Salmonella typhimurium*, and *B. subtilis, Synechocystis* and *M. mazei*. GS are in general active in a dodecameric, unmodified complex under nitrogen limitation. Upon an ammonium upshift, GS are inactivated by feedback inhibition (BcGS, *E. coli),* covalent modification (adenylylation, EcGS) or binding of (small) inactivating proteins (*Synechocystis*, BsGS). *M. mazei* GS on the contrary is regulated via the assembly of the active dodecamer upon 2-OG-binding and furthermore is strongly feedback inhibited by glutamine. (Bolay et al., 2018; Klähn et al., 2018, 2015; Stadtman, 2001; Travis et al., 2022b). Created with BioRender.com

The plasmid pRS1672 was constructed for producing untagged $GlnK_1$. The $GlnK_1$ gene was PCR-amplified using primers GlnK1_MM0732.for (5'ATGGTTGGCTATGAAATACGTAATTG3') and GlnK1_MM0732.rev (5'TCAAATTGCCTCAGGTCCG3') and cloned into pETSUMO by using the Champion™ pET SUMO Expression System (Thermo Fisher Scientific, Waltham, Massachusetts) according to the manufacturer's protocol. pRS1672 was then transformed into *E. coli* DH5α and BL21 (DE3) pRIL (suppl. Tab. S1).

Heterologous expression and protein purification: Strep-$GlnA_1$ and $GlnK_1$

Heterologous expression of Strep-$GlnA_1$-variants (pRS1841 and pRS1951) and Strep-$GlnA_1$-sP26-coexpression (pRS1841 + pRS1863) were performed in 1 l Luria Bertani medium (LB, Carl Roth GmbH + Co. KG, Karlsruhe, Germany). *E. coli* BL21 (DE3) containing pRS1841, pRS1841 and pRS1863 or pRS1951 was grown to an optical turbidity at 600 nm (T_{600}) of 0.6 - 0.8, induced with 25 µM isopropylβ-d-1-thiogalactopyranoside (IPTG, Carl Roth GmbH + Co. KG, Karlsruhe, Germany) and further incubated over night at 18 °C and 120 rpm. The cells were harvested (6,371 x g, 20 min, 4 °C) and resuspended in 6 ml W-buffer (100 mM TRIS/HCl, 150 mM NaCl, 2.5 mM EDTA, (chemicals from Carl Roth GmbH + Co. KG, Karlsruhe, Germany), 12.5 mM 2-oxoglutarate (2-OG, Sigma-Aldrich, St. Louis, Missouri), pH 8.0). After the addition of DNase I (Sigma-Aldrich, St. Louis, Missouri), cell disruption was performed twice using a French Pressure Cell at 4.135 x 10^6 N/m^2 (*Sim-Aminco Spectronic Instruments*, Dallas, Texas) followed by centrifugation of the cell lysate for (30 min (13,804 x g, 4 °C). The supernatant was incubated with 1 ml equilibrated (W-buffer) Strep-Tactin sepharose matrix (IBA, Gottingen, Germany) at 4°C for 1 h at 20 rpm. Strep-tagged $GlnA_1$ was eluted from the gravity flow column by adding E-buffer (W-buffer + 2.5 mM desthiobiotine (IBA, Gottingen, Germany)). Strep-$GlnA_1$ was always purified and stored in the presence of 12.5 mM 2-OG, either in E-buffer or 50 mM HEPES, pH 7.0 at 4 °C for a few days or with 5 % glycerol at -80 °C (chemicals from Carl Roth GmbH + Co. KG, Karlsruhe, Germany).

His_6-SUMO-$GlnK_1$ was expressed similarly using *E. coli* BL21 (DE3) pRIL + pRS1672. Expression was induced with 100 µM IPTG, incubated at 37 °C, 180 rpm for 2 h and harvested. The pellet was resuspended in phosphate buffer (50 mM phosphate, 300 mM NaCl, pH 8 (chemicals from Carl Roth GmbH + Co. KG, Karlsruhe, Germany)) and the cell extract was prepared as described above. His-tag-affinity chromatography-purifcation was performed with a Ni-NTA agarose (Qiagen, Hilden, Germany) gravity flow column, the protein was purified by stepwise-elution with 100 and 250 mM imidazole (SERVA, Heidelberg, Deutschland) in phosphate buffer. SUMO-protease (Thermo Fisher Scientific, Waltham, Massachusetts) was used according to the manufacturer's protocol to cleave the His_6-SUMO-$GlnK_1$ and obtain untagged $GlnK_1$ by passing through the Ni-NTA-column after the cleavage. Elution fractions of protein purifications were analyzed on 12 % SDS-PAGE gels and the protein concentrations were determined by Bradford (Bio-Rad Laboratories, Hercules, California) or Qubit protein assay (Thermo Fisher Sceintific, Waltham, Massachusetts).

Determination of glutamine synthetase activity

The glutamine synthetase activity was determined by performing a coupled optical assay (Shapiro and Stadtman, 1970). The assay was performed as described in Gutt et al. 2021 with modifications. First, a substrate mix containing 257 mM KCl, 143 mM NH_4Cl, 143 mM $MgCl_2$ (chemicals from Carl Roth GmbH + Co. KG, Karlsruhe, Germany) and 86 mM sodium-glutamate (Sigma-Aldrich, St. Louis, Missouri) was prepared. The assay was performed in a final volume of 1 ml including 350 µl of the substrate mix, 50 mM HEPES (final concentration, Carl Roth GmbH + Co. KG, Karlsruhe, Germany), the respective amount of 2-OG (Sigma-Aldrich, St. Louis, Missouri),, 1 mM phosphoenolpyruvate (PEP, (Sigma-Aldrich, St. Louis, Missouri), 0.42 mM nicotinamide adenine dinucleotide (NADH) and 10 or 20 µg of Strep-$GlnA_1$. After preincubation at room temperature in a volume of 950 µl for 5 min, the assay mixture was transferred to a cuvette, the time course measurement at 340 nm was started and the enzyme reaction induced by adding 3.6

mM ATP (pH adjusted to 7.0, Roche, Basel, Switzerland) (suppl. Fig. S7). The assays were performed with four technical replicates per condition, including two concentrations of GnA_1 (2 x 10 µg and 2 x 20 µg of Strep-$GlnA_1$, present in 100 µl were added). Strep-$GlnA_1$ was stored in E-buffer (described above) or 50 mM HEPES containing 12.5 mM 2-OG which was dialysed against 50 mM HEPES pH 7.0 using Amicon® Ultra catridges with 30 kDa filters (MilliporeSigma, Burlington, Massachusetts) for the enzyme assays in the absence of 2-OG.

Mass photometry

The molecular weight of protein complexes was analysed by mass photometry (MP) using a Refeyn twoMP mass photometer with the AcquireMP software (Refeyn Ltd., Oxford, UK). All measurements were performed in 50 mM HEPES, 150 mM NaCl pH 7.0 (MP-buffer, chemicals from Carl Roth GmbH + Co. KG, Karlsruhe, Germany) on 1.5 H, 24 x 60 mm microscope coverslips with Culture Well Reusable Gaskets (GRACE BIO-LABS, Bend, Oregon). Strep-$GlnA_1$ and untagged $GlnK_1$ were prepared as described above. Prior to MP experiments, a size exclusion chromatography (SEC) was performed with $GlnA_1$ in the presence of 12.5 mM 2-OG on a Superose™ 6 Increase 10/300 GL column (Cytiva, Marlborough, Massachusetts) with a flow rate of 0.5 ml/min. Only the dodecameric fraction was used for MP experiments and dialysed against MP buffer using Amicon® Ultra catridges with 30 kDa filters (MilliporeSigma, Burlington, Massachusetts) beforehand. The Gel Filtration HMW Calibration Kit (Cytiva, Marlborough, Massachusetts) was used as a standard in SEC. 75 – 200 nM monomeric Strep-$GlnA_1$ were used in the MP measurements, $GlnK_1$ was added accordingly in the desired ratio calculated based on monomers. The analysis of the acquired data was performed with the DiscoverMP software by applying a pre-measured standard (Refeyn Ltd., Oxford, UK). Counts were visualized in mass histograms as relative counts, which were calculated for the Gaussian fits of the measured peaks. For the determination of EC50-values and creating sigmoidal fitted curves, RStudio (RStudio Team (2020). RStudio: Integrated Development for R. RStudio, PBC, Boston, MA URL) was used.

Cryo-electron sample preparation and Data collection

Purified GS at a concentration of 1.5 mg/mL was rapidly applied to glow-discharged Quantifoil grids, blotted with force 4 for 3.5 s, and vitrified by directly plunging in liquid ethane (cooled by liquid nitrogen) using Vitrobot Mark IV (Thermo Fisher Scientific, Waltham, Massachusetts) at 100% humidity and 4 °C. To overcome prefererred orientation bias, 0.7 mM CHAPSO was added to prevent water-air interface interactions, consequently the concentration of the protein was increased to 6mg/ml. We added purified commercially synthesized sP26 (Davids Biotechnologie, Regensburg, Germany) to all samples, but the peptide did not stably bind under the observed conditions. Data was acquired with EPU in EER-format on an FEI Titan Krios G4 (Cryo-EM Platform, Helmholtz Munich) equipped with a Falcon IVi detector (Thermo Fisher Scientific, Waltham, Massachusetts) with a total electron dose of ~55 electrons per $Å^2$ and a pixel size of 0.76 Å. Micrographs were recorded in a defocus range of -0.25 to -2.0 µm. For details see **suppl. Table S2**.

Cryo EM - Image processing, classification and refinement

All data was processed using Cryosparc (Punjani et al., 2017). Micrographs were processed on the fly (motion correction, CTF estimation). Using blob picker, 878,308 particles were picked, 2D-classified and used for ab initio reconstruction. Iterative rounds of ab initio and heterogenous refinement were used to clean the particle stacks. The final refinements yielded models with an estimated resolution of 2.39 Å sets at the 0.143 cutoff (suppl. Fig. S3).

An initial model was generated from the protein sequences using alphaFold (Jumper et al., 2021), and thereupon fitted as rigid bodies into the density using UCSF Chimera (Pettersen et al., 2021). The model was manually rebuilt using *Coot* (Emsley et al., 2010). The final model was

subjected to real-space refinements in PHENIX (Liebschner et al., 2019). Illustrations of the models were prepared using UCSF ChimeraX (Pettersen et al., 2021). The structure is accessible under PDB: 8s59. For details see **suppl. Table S2**.

Supplementary tables and figures

Table S1

Strains and plasmids.

	Properties	Reference
Strains		
E. coli DH5α	General cloning strain	(Hanahan, 1983)
E. coli BL21 (DE3)	Strain for protein expression	Thermo Fisher Scientific, Waltham, USA
E. coli BL21 (DE3) + pRIL	Strain for protein expression of genes with unusual codons/ Cm^R	Stratagene, La Jolla, USA
Plasmids		
pET21a	General cloning vector providing a C-terminal His_6-tag	Novagen/Merck, Darmstadt, Germany
pETSUMO	Expression vector providing an N-terminal His_6-SUMO-tag	Thermo Fisher Scientific, Waltham, USA
pRS375	pET28a/Strep + $GlnA_1$	(Gutt et al., 2021)
pRS1672	pETSUMO + $GlnK_1$	This work
pRS1728	pEX-A258 + codon-optimized $GlnA_1$ and sP26	Eurofins Scientific, Ebersberg, Germany
pRS1841	pRS375 + codon-optimized $GlnA_1$	This work
pRS1863	pET21a + codon-optimized sP26	This work
pRS1951	pRS1840mut: R66A$GlnA_1$	This work

Table S2

Cryo-EM data collection, refinement and validation statistics

	Dodecamer Gln complex (EMDB- 19730) (PDB 8S59)
Data collection and processing	
Magnification	165,000 x
Voltage (kV)	300
Electron exposure (e–/Å^2)	55.0
Defocus range (μm)	0.25-2.0
Pixel size (Å)	0.72
Symmetry imposed	D6
Initial particle images (no.)	1,243,001
Final particle images (no.)	878,308
Map resolution (Å)	2.39
FSC threshold	0.143
Map resolution range (Å)	2.3-3.0
Refinement	
Initial model used (PDB code)	*de novo*, AlphaFold
Model resolution (Å)	2.5
FSC threshold	0.5
Model resolution range (Å)	2.2-2.5
Map sharpening *B* factor (Å^2)	-80.1
Model composition	
Non-hydrogen atoms	46968
Protein residues	5352
Ligands	AKG: 12
B factors (Å^2)	
Protein	16.58
Ligand	15.64
R.m.s. deviations	
Bond lengths (Å)	0.003
Bond angles (°)	0.602
Validation	
MolProbity score	1.29
Clashscore	5.32
Poor rotamers (%)	0.46
Ramachandran plot	
Favored (%)	98.22
Allowed (%)	1.56
Disallowed (%)	0.23

Suppl. Figure S1

Affinity-purified Strep-GlnA$_1$ and size-exclusion-chromatography (SEC) and MP of Strep-GlnA$_1$ after purification.

A: 1.5 µg (lane 1) and 3 µg (lane 2) Strep-GlnA$_1$ on a coomassie-stained 12 % SDS-Gel. **B**: Elution profile of Strep-GlnA$_1$ (black) and size standard (dashed line, molecular weights in italics). Size exclusion chromatography was performed on a Superose™ 6 Increase 10/300 GL column (Cytiva, Marlborough, USA) with a flow rate of 0.5 ml/min in the presence of 12.5 mM 2-OG. **C:** Mass photometry spectrum of Strep-GlnA$_1$ after SEC in 12.5 mM 2-OG.

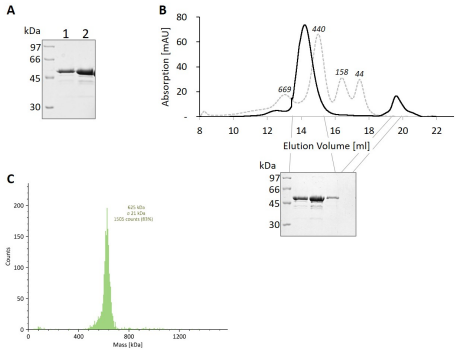

Suppl. Figure S2

Sigmoidal fitted curves for mass photometry measurements of Strep-GlnA$_1$ with varying concentrations of 2-OG.

The curves were fitted and EC50-values calculated using RStudio (RStudio Team (2020). RStudio: Integrated Development for R. RStudio, PBC, Boston, MA URL). **A, B**: Two replicates for 2-OG titration, formation of dodecamer is shown in percent. **C, D**: 2-OG titration in the absence (C) and presence of GlnK$_1$ (D), formation of dodecamer/dimer.

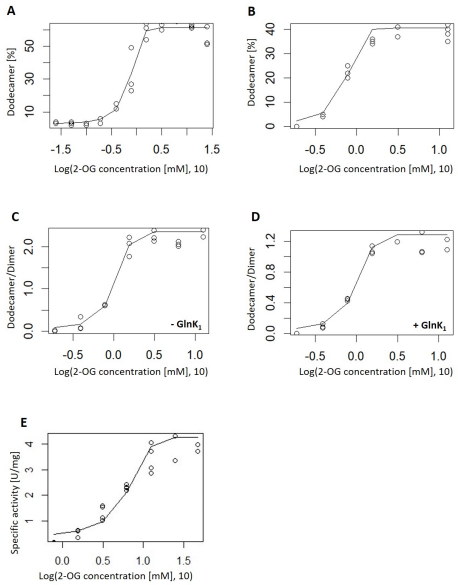

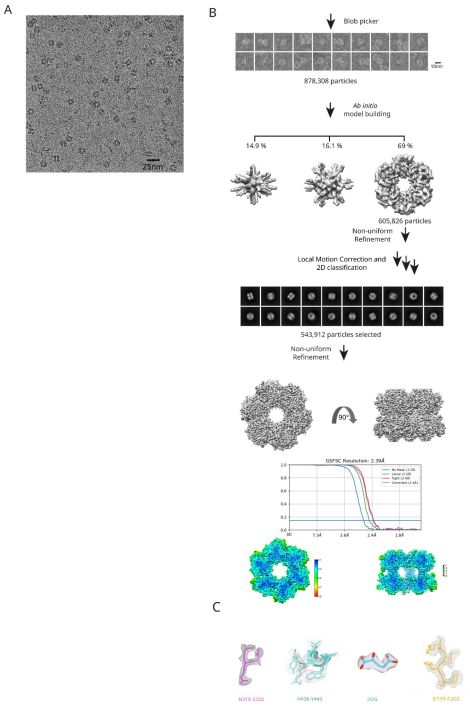

Suppl. Figure S3

Cryo-EM Data processing workflow.

A: Representative motion-corrected micrograph showing different orientations of the $GlnA_1$ particles **B**: Cryo-EM processing tree used for obtaining the high-resolution structure of $GlnA_1$. The map obtained is coloured by resolution, where the global resolution was estimated using GSFSC **C**: Different regions of $GlnA_1$ encased around the cryo-EM density.

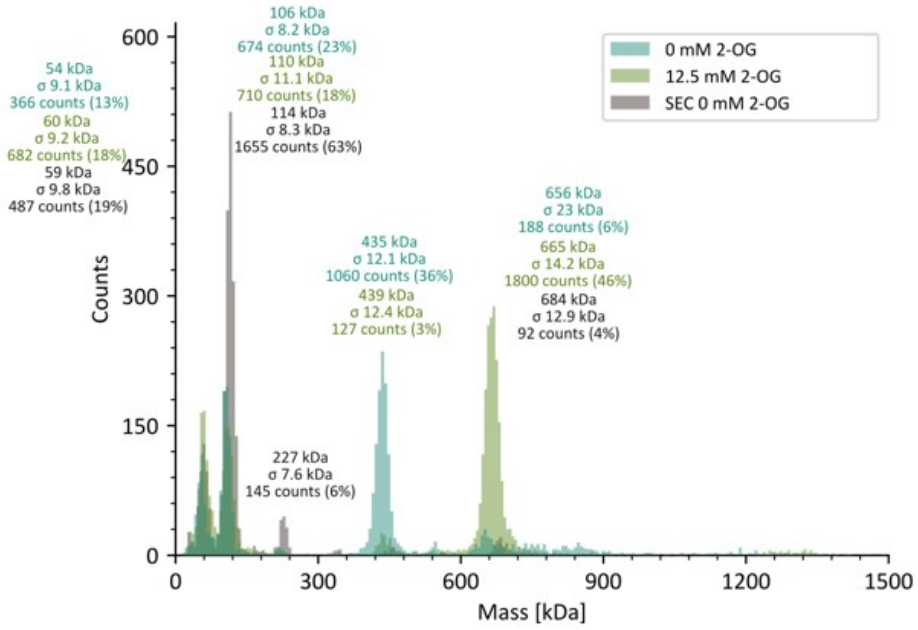

Suppl. Figure S4

Mass photometry of purified and thawed Strep-GlnA$_1$ before and after SEC.

Mass spectra of Strep-GlnA$_1$ samples with 0 and 12.5 mM after affinity-purification (blue ●, 0 mM and green ●, 12.5 mM 2-OG) and after SEC (0 mM 2-OG, grey ●).

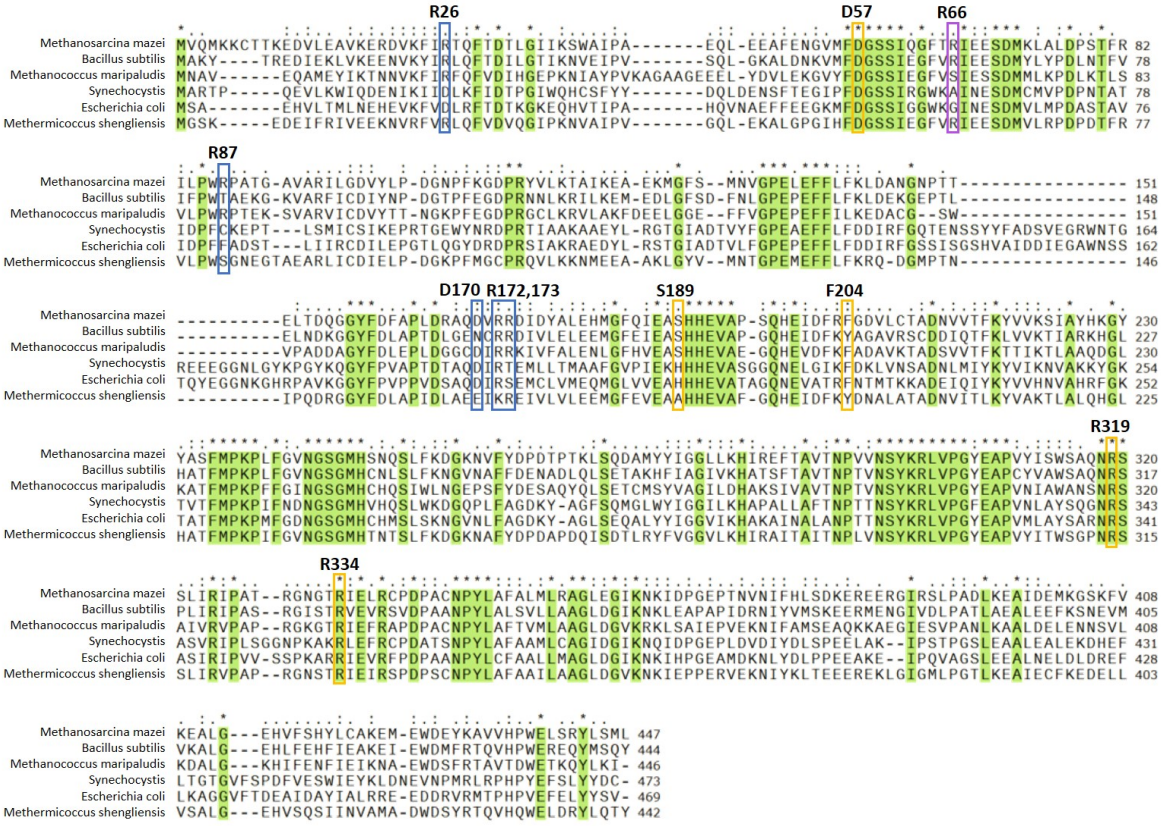

Suppl. Figure S5

Amino-acid sequence alignment of different model organism glutamine synthetases.

(Alignment tool: COBALT, visualization in SnapGene) Conserved amino-acids are highlighted in green. The relevant residues in *M. mazei* for 2-OG- and substrate-binding, as well as the arginine responsible for the feedback inhibition by glutamine are highlighted by coloured boxes (blue ●, orange ● and purple ●, respectively).

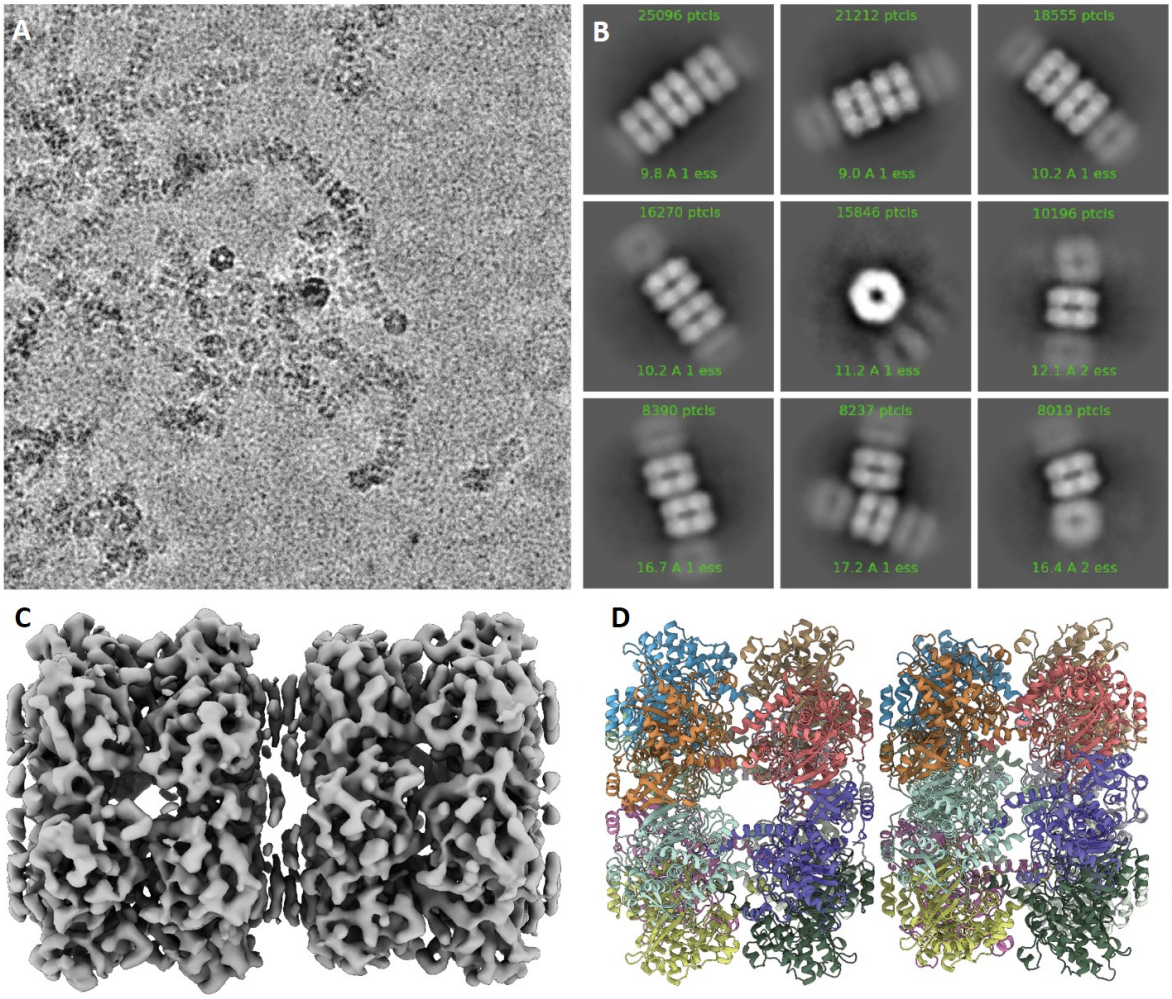

Suppl. Figure S6

M. mazei $GlnA_1$ filaments.

A: Representative motion-corrected micrograph showing $GlnA_1$ filaments **B**: Reference-free 2D classes showcasing filament orientations **C, D**: 3D reconstructed map of $GlnA_1$ filament and its model.

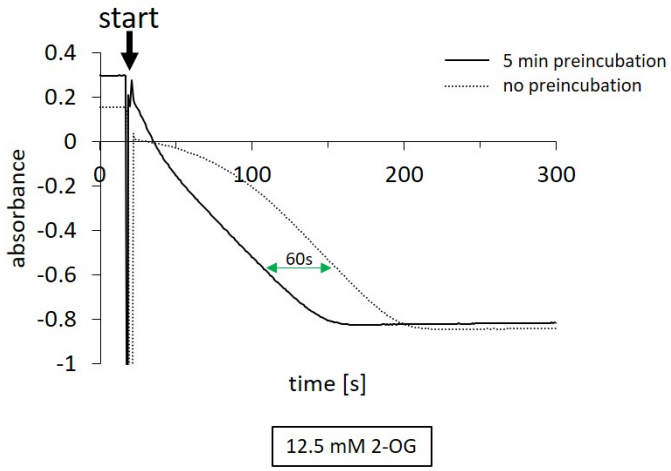

Suppl. Figure S7

Original kinetic assay of Strep-GlnA$_1$ in the presence of 12.5 mM 2-OG.

Measurements with and without pre-incubation of GlnA$_1$ in the presence of 12.5 mM 2-OG are shown.

Acknowledgements

We thank the members of our laboratories for useful discussions on the experiments, as well as Claudia Kiessling for technical assistance. This work was supported by the German Research Council (DFG) priority program (SPP) 2002 'Small proteins in Prokaryotes, an unexplored world' [Schm1052/20-2]. We acknowledge the contribution of the CryoEM Facility of the Philipps University of Marburg. J.M.S. acknowledges the DFG for an Emmy Noether grant (SCHU 3364/1-1) cofunded by the European Union (ERC, TwoCO2One, 101075992). Views and opinions expressed are, however, those of the author(s) only and do not necessarily reflect those of the European Union or the European Research Council. Neither the European Union nor the granting authority can be held responsible for them. We thank Sandra Schuller for useful discussions and help in preparing manuscript figures. GKAH was supported by the Max Planck Society. We acknowledge financial support by Land Schleswig-Holstein within the funding programme Open Access Publikationsfonds.

Additional files

Validation report cryo-EM

References

Almassy R.J., Janson C.A., Hamlin R., Xuong N.-H., Eisenberg D 1986) **Novel subunit—subunit interactions in the structure of glutamine synthetase** *Nature* **323**:304–309 https://doi.org/10.1038/323304a0

Bolay P., Muro-Pastor M.I., Florencio F.J., Klähn S 2018) **The Distinctive Regulation of Cyanobacterial Glutamine Synthetase** *Life* **8**:52 https://doi.org/10.3390/life8040052

Brown J.R., Masuchi Y., Robb F.T., Doolittlel W.F 1994) **Evolutionary relationships of bacterial and archaeal glutamine synthetase genes** *J. Mol. Evol* **38**:566–576 https://doi.org/10.1007/BF00175876

Cohen-Kupiec R., Marx C.J., Leigh J.A 1999) **Function and regulation of glnA in the methanogenic archaeon Methanococcus maripaludis** *J. Bacteriol* **181**:256–261 https://doi.org/10.1128/JB.181.1.256-261.1999

Deuel T.F., Ginsburg A., Yeh J., Shelton E., Stadtman E.R 1970) **Bacillus subtilis glutamine synthetase. Purification and physical characterization** *J. Biol. Chem* **245**:5195–5205

Dos Santos Moreira C.D., Ramos M.J.R.N., Fernandes P.M.A.A. 2019) **Glutamine synthetase structure-catalysis relationship—Recent advances and applications** *WIREs Comput. Mol. Sci* **9**:e1399 https://doi.org/10.1002/wcms.1399

Ehlers C., Weidenbach K., Veit K., Forchhammer K., Schmitz R.A 2005) **Unique mechanistic features of post-translational regulation of glutamine synthetase activity in Methanosarcina mazei strain Gö1 in response to nitrogen availability: Regulation of glutamine synthetase activity in M. mazei** *Mol. Microbiol* **55**:1841–1854 https://doi.org/10.1111/j.1365-2958.2005.04511.x

Emsley P., Lohkamp B., Scott W.G., Cowtan K 2010) **Features and development of Coot** *Acta Crystallogr. D Biol. Crystallogr* **66**:486–501 https://doi.org/10.1107/S0907444910007493

Fedorova K., Kayumov A., Woyda K., Ilinskaja O., Forchhammer K 2013) **Transcription factor TnrA inhibits the biosynthetic activity of glutamine synthetase in Bacillus subtilis** *FEBS Lett* **587**:1293–1298 https://doi.org/10.1016/j.febslet.2013.03.015

Fisher S.H 1999) **Regulation of nitrogen metabolism in Bacillus subtilis: vive la différence! Mol** *Microbiol* **32**:223–232 https://doi.org/10.1046/j.1365-2958.1999.01333.x

Fisher S.H., Wray L.V 2008) **Bacillus subtilis glutamine synthetase regulates its own synthesis by acting as a chaperone to stabilize GlnR-DNA complexes** *Proc. Natl. Acad. Sci. U. S. A* **105**:1014–1019 https://doi.org/10.1073/pnas.0709949105

Forchhammer K., Peschek G.A., Löffelhardt W., Schmetterer G. 1999) **The PII Protein in Synechococcus PCC 7942 Senses and Signals 2-Oxoglutarate Under ATP-Replete Conditions** *The Phototrophic Prokaryotes* Boston, MA: Springer US :549–553 https://doi.org/10.1007/978-1-4615-4827-0_63

García-Domínguez M., Reyes J.C., Florencio F.J 1999) **Glutamine synthetase inactivation by protein–protein interaction** *Proc. Natl. Acad. Sci* **96**:7161–7166 https://doi.org/10.1073/pnas.96.13.7161

Gunka K., Commichau F.M 2012) **Control of glutamate homeostasis in Bacillus subtilis: a complex interplay between ammonium assimilation, glutamate biosynthesis and degradation** *Mol. Microbiol* **85**:213–224 https://doi.org/10.1111/j.1365-2958.2012.08105.x

Gutt M., Jordan B., Weidenbach K., Gudzuhn M., Kiessling C., Cassidy L., Helbig A., Tholey A., Pyper D.J., Kubatova N., Schwalbe H., Schmitz R.A 2021) **High complexity of Glutamine synthetase regulation in Methanosarcina mazei: Small protein 26 interacts and enhances glutamine synthetase activity** *Febs J.* https://doi.org/10.1111/febs.15799

Hanahan D 1983) **Studies on transformation of Escherichia coli with plasmids** *J. Mol. Biol* **166**:557–580 https://doi.org/10.1016/s0022-2836(83)80284-8

Hauf K., Kayumov A., Gloge F., Forchhammer K 2016) **The Molecular Basis of TnrA Control by Glutamine Synthetase in Bacillus subtilis*** *J. Biol. Chem* **291**:3483–3495 https://doi.org/10.1074/jbc.M115.680991

He Y.-X., Gui L., Liu Y.-Z., Du Y., Zhou Y., Li P., Zhou C.-Z 2009) **Crystal structure of Saccharomyces cerevisiae glutamine synthetase Gln1 suggests a nanotube-like supramolecular assembly** *Proteins Struct. Funct. Bioinforma* **76**:249–254 https://doi.org/10.1002/prot.22403

Herrero A., Muro-Pastor A.M., Flores E 2001) **Nitrogen Control in Cyanobacteria** *J. Bacteriol* **183**:411–425 https://doi.org/10.1128/jb.183.2.411-425.2001

Huang P.-C., Chen S.-K., Chiang W.-H., Ho M.-R., Wu K.-P 2022) **Structural basis for the helical filament formation of Escherichia coli glutamine synthetase** *Protein Sci* **31**:e4304 https://doi.org/10.1002/pro.4304

Inoue H., Nojima H., Okayama H 1990) **High efficiency transformation of Escherichia coli with plasmids** *Gene* **96**:23–28 https://doi.org/10.1016/0378-1119(90)90336-p

Jäger D., Sharma C.M., Thomsen J., Ehlers C., Vogel J., Schmitz R.A 2009) **Deep sequencing analysis of the Methanosarcina mazei Gö1 transcriptome in response to nitrogen availability** *Proc. Natl. Acad. Sci* **106**:21878–21882 https://doi.org/10.1073/pnas.0909051106

Jiang P., Peliska J.A., Ninfa A.J 1998) **Reconstitution of the signal-transduction bicyclic cascade responsible for the regulation of Ntr gene transcription in Escherichia coli** *Biochemistry* **37**:12795–12801 https://doi.org/10.1021/bi9802420

Jumper J., Evans R., Pritzel A., Green T., Figurnov M., Ronneberger O., Tunyasuvunakool K., Bates R., Žídek A., Potapenko A., Bridgland A., Meyer C., Kohl S.A.A., Ballard A.J., Cowie A., Romera-Paredes B., Nikolov S., Jain R., Adler J., Back T., Petersen S., Reiman D., Clancy E., Zielinski M., Steinegger M., Pacholska M., Berghammer T., Bodenstein S., Silver D., Vinyals O., Senior A.W., Kavukcuoglu K., Kohli P., Hassabis D. 2021) **Highly accurate protein structure prediction with AlphaFold** *Nature* **596**:583–589 https://doi.org/10.1038/s41586-021-03819-2

Klähn S., Bolay P., Wright P.R., Atilho R.M., Brewer K.I., Hagemann M., Breaker R.R., Hess W.R 2018) **A glutamine riboswitch is a key element for the regulation of glutamine synthetase in cyanobacteria** *Nucleic Acids Res* https://doi.org/10.1093/nar/gky709

Klähn S., Schaal C., Georg J., Baumgartner D., Knippen G., Hagemann M., Muro-Pastor A.M., Hess W.R 2015) **The sRNA NsiR4 is involved in nitrogen assimilation control in cyanobacteria by targeting glutamine synthetase inactivating factor IF7** *Proc. Natl. Acad. Sci* **112** https://doi.org/10.1073/pnas.1508412112

Legrain C., Vissers S., Dubois E., Legrain M., Wiame J.-M 1982) **Regulation of Glutamine Synthetase from Saccharomyces cerevisiae by Repression, Inactivation and Proteolysis** *Eur. J. Biochem* **123**:611–616 https://doi.org/10.1111/j.1432-1033.1982.tb06576.x

Liaw S.H., Eisenberg D 1994) **Structural model for the reaction mechanism of glutamine synthetase, based on five crystal structures of enzyme-substrate complexes** *Biochemistry* **33**:675–681 https://doi.org/10.1021/bi00169a007

Liaw S.H., Pan C., Eisenberg D 1993) **Feedback inhibition of fully unadenylylated glutamine synthetase from Salmonella typhimurium by glycine, alanine, and serine** *Proc. Natl. Acad. Sci. U. S. A* **90**:4996–5000 https://doi.org/10.1073/pnas.90.11.4996

Lie T.J., Dodsworth J.A., Nickle D.C., Leigh J.A 2007) **Diverse homologues of the archaeal repressor NrpR function similarly in nitrogen regulation** *FEMS Microbiol. Lett* **271**:281–288 https://doi.org/10.1111/j.1574-6968.2007.00726.x

Liebschner D., Afonine P.V., Baker M.L., Bunkóczi G., Chen V.B., Croll T.I., Hintze B., Hung L.-W., Jain S., McCoy A.J., Moriarty N.W., Oeffner R.D., Poon B.K., Prisant M.G., Read R.J., Richardson J.S., Richardson D.C., Sammito M.D., Sobolev O.V., Stockwell D.H., Terwilliger T.C., Urzhumtsev A.G., Videau L.L., Williams C.J., Adams P.D 2019) **Macromolecular structure determination using X-rays, neutrons and electrons: recent developments in Phenix** *Acta Crystallogr. Sect. Struct. Biol* **75**:861–877 https://doi.org/10.1107/S2059798319011471

Magasanik B 1993) **The regulation of nitrogen utilization in enteric bacteria** *J. Cell. Biochem* **51**:34–40 https://doi.org/10.1002/jcb.240510108

Masalkar P.D., Roberts D.M 2015) **Glutamine synthetase isoforms in nitrogen-fixing soybean nodules: distinct oligomeric structures and thiol-based regulation** *FEBS Lett* **589**:215–221 https://doi.org/10.1016/j.febslet.2014.11.048

Müller M.-C., Lemaire O.N., Kurth J.M., Welte C.U., Wagner T 2024) **Differences in regulation mechanisms of glutamine synthetases from methanogenic archaea unveiled by structural investigations. Commun** *Biol* **7**:1–14 https://doi.org/10.1038/s42003-023-05726-w

Murray D.S., Chinnam N., Tonthat N.K., Whitfill T., Wray L.V., Fisher S.H., Schumacher M.A 2013) **Structures of the Bacillus subtilis glutamine synthetase dodecamer reveal large intersubunit catalytic conformational changes linked to a unique feedback inhibition mechanism** *J. Biol. Chem* **288**:35801–35811 https://doi.org/10.1074/jbc.M113.519496

Pedro-Roig L., Camacho M., Bonete M.-J 2013) **Regulation of ammonium assimilation in Haloferax mediterranei: interaction between glutamine synthetase and two GlnK proteins** *Biochim. Biophys. Acta* **1834**:16–23 https://doi.org/10.1016/j.bbapap.2012.10.006

Petrovska I., Nüske E., Munder M.C., Kulasegaran G., Malinovska L., Kroschwald S., Richter D., Fahmy K., Gibson K., Verbavatz J.-M., Alberti S 2014) **Filament formation by metabolic enzymes is a specific adaptation to an advanced state of cellular starvation** *eLife* **3**:e02409 https://doi.org/10.7554/eLife.02409

Pettersen E.F., Goddard T.D., Huang C.C., Meng E.C., Couch G.S., Croll T.I., Morris J.H., Ferrin T.E 2021) **UCSF ChimeraX: Structure visualization for researchers, educators, and developers** *Protein Sci. Publ. Protein Soc* **30**:70–82 https://doi.org/10.1002/pro.3943

Prasse D., Schmitz R.A. 2018) **Small RNAs Involved in Regulation of Nitrogen Metabolism** *Microbiol. Spectr* **6** https://doi.org/10.1128/microbiolspec.RWR-0018-2018

Punjani A., Rubinstein J.L., Fleet D.J., Brubaker M.A 2017) **cryoSPARC: algorithms for rapid unsupervised cryo-EM structure determination** *Nat. Methods* **14**:290–296 https://doi.org/10.1038/nmeth.4169

Reitzer L 2003) **Nitrogen Assimilation and Global Regulation in Escherichia coli** *Annu. Rev. Microbiol* **57**:155–176 https://doi.org/10.1146/annurev.micro.57.030502.090820

Schumacher M.A., Salinas R., Travis B.A., Singh R.R., Lent N 2023) **M. mazei glutamine synthetase and glutamine synthetase-GlnK1 structures reveal enzyme regulation by oligomer modulation** *Nat. Commun* **14**:7375 https://doi.org/10.1038/s41467-023-43243-w

Shapiro B.M., Stadtman E.R. 1970) **[130] Glutamine synthetase (Escherichia coli)** *Methods in Enzymology* Elsevier :910–922 https://doi.org/10.1016/0076-6879(71)17305-3

Stadtman E.R 2004) **Regulation of Glutamine Synthetase Activity** *EcoSal Plus* **1** https://doi.org/10.1128/ecosalplus.3.6.1.6

Stadtman E.R 2001) **The story of glutamine synthetase regulation** *J. Biol. Chem* **276**:44357–44364 https://doi.org/10.1074/jbc.R100055200

Stadtman E.R., Deutscher M.P. 1990) **[60] Discovery of glutamine synthetase cascade** *Methods in Enzymology, Guide to Protein Purification* Academic Press :793–809 https://doi.org/10.1016/0076-6879(90)82062-7

Travis B.A., Peck J.V., Salinas R., Dopkins B., Lent N., Nguyen V.D., Borgnia M.J., Brennan R.G., Schumacher M.A 2022b) **Molecular dissection of the glutamine synthetase-GlnR nitrogen regulatory circuitry in Gram-positive bacteria** *Nat. Commun* **13**:3793 https://doi.org/10.1038/s41467-022-31573-0

Valentine R.C., Shapiro B.M., Stadtman E.R 1968) **Regulation of glutamine synthetase** *XII. Electron microscopy of the enzyme from Escherichia coli. Biochemistry* **7**:2143–2152 https://doi.org/10.1021/bi00846a017

van Heeswijk W.C., Westerhoff H.V., Boogerd F.C. 2013) **Nitrogen Assimilation in Escherichia coli: Putting Molecular Data into a Systems Perspective** *Microbiol. Mol. Biol. Rev* **77**:628–695 https://doi.org/10.1128/mmbr.00025-13

van Rooyen J.M., Abratt V.R., Belrhali H., Sewell T. 2011) **Crystal structure of Type III glutamine synthetase: surprising reversal of the inter-ring interface** *Struct. Lond. Engl* **1993**:471–483 https://doi.org/10.1016/j.str.2011.02.001

Veit K., Ehlers C., Schmitz R.A 2005) **Effects of nitrogen and carbon sources on transcription of soluble methyltransferases in Methanosarcina mazei strain Go1** *J. Bacteriol* **187**:6147–6154 https://doi.org/10.1128/JB.187.17.6147-6154.2005

Weidenbach K., Ehlers C., Kock J., Ehrenreich A., Schmitz R.A 2008) **Insights into the NrpR regulon in Methanosarcina mazei Gö1** *Arch. Microbiol* **190**:319–332 https://doi.org/10.1007

/s00203-008-0369-3

Weidenbach K., Ehlers C., Kock J., Schmitz R.A 2010) **NrpRII mediates contacts between NrpRI and general transcription factors in the archaeon Methanosarcina mazei Gö1** *Febs J* **277**:4398–4411 https://doi.org/10.1111/j.1742-4658.2010.07821.x

Wisedchaisri G., Dranow D.M., Lie T.J., Bonanno J.B., Patskovsky Y., Ozyurt S.A., Sauder J.M., Almo S.C., Wasserman S.R., Burley S.K., Leigh J.A., Gonen T 2010) **Structural Underpinnings of Nitrogen Regulation by the Prototypical Nitrogen-Responsive Transcriptional Factor NrpR** *Structure* **18**:1512–1521 https://doi.org/10.1016/j.str.2010.08.014

Woolfolk C.A., Stadtman E.R 1967) **Regulation of glutamine synthetase: III. Cumulative feedback inhibition of glutamine synthetase from Escherichia coli** *Arch. Biochem. Biophys* **118**:736–755 https://doi.org/10.1016/0003-9861(67)90412-2

Yamashita M., Almassy R., Janson C., Cascio D., Eisenberg D 1989) **Refined atomic model of glutamine synthetase at 3.5 Å resolution** *J. Biol. Chem* **264**:17681–90 https://doi.org/10.2210/pdb2gls/pdb

Author information

Eva Herdering[+]
Institute for General Microbiology, Christian Albrechts University, Kiel, Germany

[+]authors contributed equally

Tristan Reif-Trauttmansdorff[+]
Center for Synthetic Microbiology (SYNMIKRO) Research Center and Department of Chemistry, Philipps-Universität Marburg, Marburg, Germany

[+]authors contributed equally

Anuj Kumar
Center for Synthetic Microbiology (SYNMIKRO) Research Center and Department of Chemistry, Philipps-Universität Marburg, Marburg, Germany

Tim Habenicht
Institute for General Microbiology, Christian Albrechts University, Kiel, Germany

Georg Hochberg
Center for Synthetic Microbiology (SYNMIKRO) Research Center and Department of Chemistry, Philipps-Universität Marburg, Marburg, Germany, Evolutionary Biochemistry Group, Max Planck Institute for Terrestrial Microbiology, Marburg, Germany, Department of Chemistry, Philipps-Universität Marburg, Marburg, Germany

Stefan Bohn
Cryo-Electron Microscopy Platform and Institute of Structural Biology, Helmholtz Munich, Neuherberg, Germany

Jan Schuller
Center for Synthetic Microbiology (SYNMIKRO) Research Center and Department of Chemistry, Philipps-Universität Marburg, Marburg, Germany

For correspondence: jan.schuller@synmikro.uni-marburg.de

Ruth A Schmitz
Institute for General Microbiology, Christian Albrechts University, Kiel, Germany
ORCID iD: 0000-0002-6788-0829

For correspondence: rschmitz@ifam.uni-kiel.de

Editors

Reviewer #1 (Public review):

Summary:

Shows a new mechanism of GS regulation in the archaean Methanosarcina maze and clarifies the direct activation of GS activity by 2-oxoglutarate, thus featuring an other way, how 2-oxoglutarate acts as a central status reporter of C/N sensing.

Strengths:

mass photometry reveals a a dynamic mode the effect of 2-OG on the oligomerization state of GS. Single particle Cryo-EM reveals the mechanism of 2-OG mediated dodecamer formation.

Weaknesses:

Not entirely clear, how very high 2-OG concentrations activate GS beyond dodecamer formation.

In the revised version, most of my concerns were adequately addressed. In the summary it is stated that glutamine acts as allosteric inhibitor of dodecameric GS. This is not correct: glutamine binds to the active site and is therefore not allosteric. This way of feedback inhibition is a type of product inhibition

https://doi.org/10.7554/eLife.97484.2.sa3

Reviewer #2 (Public review):

Summary:

Herdering et al. introduced research on an archaeal glutamine synthetase (GS) from Methanosarcina mazei, which exhibits sensitivity to the environmental presence of 2-oxoglutarate (2-OG). While previous studies have indicated 2-OG's ability to enhance GS

activity, the precise underlying mechanism remains unclear. Initially, the authors utilized biophysical characterization, primarily employing a nanomolar-scale detection method called mass photometry, to explore the molecular assembly of Methanosarcina mazei GS (M. mazei GS) in the absence or presence of 2-OG. Similar to other GS enzymes, the target M. mazei GS forms a stable dodecamer, with two hexameric rings stacked in tail-to-tail interactions. Despite approximately 40% of M. mazei GS existing as monomeric or dimeric entities in the detectable solution, the majority spontaneously assemble into a dodecameric state. Upon mixing 2-OG with M. mazei GS, the population of the dodecameric form increases proportionally with the concentration of 2-OG, indicating that 2-OG either promotes or stabilizes the assembly process. The cryo-electron microscopy (cryo-EM) structure reveals that 2-OG is positioned near the interface of two hexameric rings. At a resolution of 2.39 Å, the cryo-EM map vividly illustrates 2-OG forming hydrogen bonds with two individual GS subunits as well as with solvent water molecules. Moreover, local sidechain reorientation and conformational changes of loops in response to 2-OG further delineate the 2-OG-stabilized assembly of M. mazei GS.

Strengths & Weaknesses:

The investigation studies into the impact of 2-oxoglutarate (2-OG) on the assembly of Methanosarcina mazei glutamine synthetase (M mazei GS). Utilizing cutting-edge mass photometry, the authors scrutinized the population dynamics of GS assembly in response to varying concentrations of 2-OG. Notably, the findings demonstrate a promising and straightforward correlation, revealing that dodecamer formation can be stimulated by 2-OG concentrations of up to 10 mM, although GS assembly never reaches 100% dodecamerization in this study. Furthermore, catalytic activities showed a remarkable enhancement, escalating from 0.0 U/mg to 7.8 U/mg with increasing concentrations of 2-OG, peaking at 12.5 mM. However, an intriguing gap arises between the incomplete dodecameric formation observed at 10 mM 2-OG, as revealed by mass photometry, and the continued increase in activity from 5 mM to 10 mM 2-OG for M mazei GS. This prompts questions regarding the inability of M mazei GS to achieve complete dodecamer formation and the underlying factors that further enhance GS activity within this concentration range of 2-OG.

Moreover, the cryo-electron microscopy (cryo-EM) analysis provides additional support for the biophysical and biochemical characterization, elucidating the precise localization of 2-OG at the interface of two GS subunits within two hexameric rings. The observed correlation between GS assembly facilitated by 2-OG and its catalytic activity is substantiated by structural reorientations at the GS-GS interface, confirming the previously reported phenomenon of "funnel activation" in GS. However, the authors did not present the cryo-EM structure of M. mazei GS in complex with ATP and glutamate in the presence of 2-OG, which could have shed light on the differences in glutamine biosynthesis between previously reported GS enzymes and the 2-OG-bound M. mazei GS.

Furthermore, besides revealing the cryo-EM structure of 2-OG-bound GS, the study also observed the filamentous form of GS, suggesting that filament formation may be a universal stacking mechanism across archaeal and bacterial species. However, efforts to enhance resolution to investigate whether the stacked polymer is induced by 2-OG or other factors such as ions or metabolites were not undertaken by the authors, leaving room for further exploration into the mechanisms underlying filament formation in GS.

Comments on revisions:

My comments have been addressed adequately.

I recognize that determining the structure of the GS complex bound to ATP and/or other ligands would enhance this study by offering a more comprehensive understanding of 2-

oxoglutarate-mediated dodecameric assembly and activation. However, I accept the authors' explanation for not including this aspect in the current work.

https://doi.org/10.7554/eLife.97484.2.sa2

Reviewer #3 (Public review):

The current manuscript investigates the effect of 2-oxoglutarate (2OG) as modulator of glutamine synthetase (GS). To do this, the authors rely of mass photometry, specific activity measurements and single particle cryo-EM data.
From the results, the authors conclude that the GS from Methanosarcina mazei shifts from a dimeric, non-active state under low concentrations of 2OG, to a dodecameric and fully active complex at saturating concentrations of 2OG.

GS is a crucial enzyme in all domains of life. The dodecameric fold of GS is recurrent amongst prokaryotic and archaea organisms but the enzyme activity can be regulated in distinct ways. This is a very interesting work combining protein biochemistry with structural biology.

A novel role for 2OG is presented for this mesophilic methanoarchaeon, as a crucial effector for the enzyme oligomerization and full reactivity.

The conclusions of this paper are mostly well supported by data, but some aspects of this GS regulation and interaction with known partners like Glnk1 and sp26 need to be clarified and extended.

https://doi.org/10.7554/eLife.97484.2.sa1

Author response:

The following is the authors' response to the original reviews.

> ***Reviewer #1 (Public Review):***
>
> *Summary:*
>
> *his study shows a new mechanism of GS regulation in the archaean Methanosarcina mazei and clarifies the direct activation of GS activity by 2-oxoglutarate, thus featuring another way in which 2-oxoglutarate acts as a central status reporter of C/N sensing.*
>
> *Mass photometry and single particle cryoEM structure analysis convincingly show the direct regulation of GS activity by 2-OG promoted formation of the dodecameric structure of GS. The previously recognized small proteins GlnK1 and Sp26 seem to play a subordinate role in GS regulation, which is in good agreement with previous data. Although these data are quite clear now, there remains one major open question: how does 2-OG further increase GS activity once the full dodecameric state is achieved (at 5 mM)? This point needs to be reconsidered.*
>
> *Weaknesses:*
>
> *It is not entirely clear, how very high 2-OG concentrations activate GS beyond dodecamer formation.*
>
> *The data presented in this work are in stark contrast to the previously reported structure of M. mazei GS by the Schumacher lab. This is very confusing for the scientific community and requires clarification. The discussion should consider possible reasons for the contradictory results.*

> *Importantly, it is puzzling how Schumacher could achieve an apo-structire of dodecameric GS? If 2-OG is necessary for dodecameric formation, this should be discussed. If GlnK1 doesn't form a complex with the dodecameric GS, how could such a complex be resolved there?*
>
> *In addition, the text is in principle clear but could be improved by professional editing. Most obviously there is insufficient comma placement.*

We thank Reviewer #1 for the professional evaluation and raising important points. We will address those comments in the updated manuscript and especially improve the discussion in respect to the two points of concern.

(1) How can GlnA1 activity further be stimulated with further increasing 2-OG after the dodecamer is already fully assembled at 5 mM 2-OG.

We assume a two-step requirement for 2-OG, the dodecameric assembly and the priming of the active sites. The assembly step is based on cooperative effects of 2-OG and does not require the presence of 2-OG in all 2-OG-binding pockets: 2-OG-binding to one binding pocket also causes a domino effect of conformational changes in the adjacent 2-OG-unbound subunit, as also described for *Methanothermococcus thermolithotrophicus* GS in Müller et al. 2023. Due to the introduction of these conformational changes, the dodecameric form becomes more favourable even without all 2-OG binding sites being occupied. With higher 2-OG concentrations present (> 5mM), the activity increased further until finally all 2-OG-binding pockets were occupied, resulting in the priming of all active sites (all subunits) and thereby reaching the maximal activity.

(2) The contradictory results with previously published data on the structure of *M. mazei* by Schumacher et al. 2023.

We certainly agree that it is confusing that Schumacher et al. 2023 obtained a dodecameric structure without the addition of 2-OG, which we claim to be essential for the dodecameric form. 2-OG is a cellular metabolite that is naturally present in *E. coli*, the heterologous expression host both groups used. Since our main question focused on analysing the 2-OG effect on GS, we have performed thorough dialysis of the purified protein to remove all 2-OG before performing MP experiments. In the absence of 2-OG we never observed significant enzyme activity and always detected a fast disassembly after incubation on ice. We thus assume that a dodecamer without 2-OG in Schumacher et al. 2023 is an inactive oligomer of a once 2-OG-bound form, stabilized e.g. by the presence of 5 mM MgCl2.

The GlnA1-GlnK1-structure (crystallography) by Schumacher et al. 2023 is in stark contrast to our findings that GlnK1 and GlnA1 do not interact as shown by mass photometry with purified proteins. A possible reason for this discrepancy might be that at the high protein concentrations used in the crystallization assay, complexes are formed based on hydrophobic or ionic protein interactions, which would not form under physiological concentrations.

> *Reviewer #2 (Public Review):*
>
> *Summary:*
>
> *Herdering et al. introduced research on an archaeal glutamine synthetase (GS) from Methanosarcina mazei, which exhibits sensitivity to the environmental presence of 2-oxoglutarate (2-OG). While previous studies have indicated 2-OG's ability to enhance GS activity, the precise underlying mechanism remains unclear. Initially, the authors utilized biophysical characterization, primarily employing a nanomolar-scale detection method called mass photometry, to explore the molecular assembly of Methanosarcina mazei GS (M. mazei GS) in the absence or presence of 2-OG. Similar to other GS enzymes, the target*

M. mazei GS forms a stable dodecamer, with two hexameric rings stacked in tail-to-tail interactions. Despite approximately 40% of M. mazei GS existing as monomeric or dimeric entities in the detectable solution, the majority spontaneously assemble into a dodecameric state. Upon mixing 2-OG with M. mazei GS, the population of the dodecameric form increases proportionally with the concentration of 2-OG, indicating that 2-OG either promotes or stabilizes the assembly process. The cryo-electron microscopy (cryo-EM) structure reveals that 2-OG is positioned near the interface of two hexameric rings. At a resolution of 2.39 Å, the cryo-EM map vividly illustrates 2-OG forming hydrogen bonds with two individual GS subunits as well as with solvent water molecules. Moreover, local side-chain reorientation and conformational changes of loops in response to 2-OG further delineate the 2-OG-stabilized assembly of M. mazei GS.

Strengths & Weaknesses:

The investigation studies the impact of 2-oxoglutarate (2-OG) on the assembly of Methanosarcina mazei glutamine synthetase (M mazei GS). Utilizing cutting-edge mass photometry, the authors scrutinized the population dynamics of GS assembly in response to varying concentrations of 2-OG. Notably, the findings demonstrate a promising and straightforward correlation, revealing that dodecamer formation can be stimulated by 2-OG concentrations of up to 10 mM, although GS assembly never reaches 100% dodecamerization in this study. Furthermore, catalytic activities showed a remarkable enhancement, escalating from 0.0 U/mg to 7.8 U/mg with increasing concentrations of 2-OG, peaking at 12.5 mM. However, an intriguing gap arises between the incomplete dodecameric formation observed at 10 mM 2-OG, as revealed by mass photometry, and the continued increase in activity from 5 mM to 10 mM 2-OG for M mazei GS. This prompts questions regarding the inability of M mazei GS to achieve complete dodecamer formation and the underlying factors that further enhance GS activity within this concentration range of 2-OG.

Moreover, the cryo-electron microscopy (cryo-EM) analysis provides additional support for the biophysical and biochemical characterization, elucidating the precise localization of 2-OG at the interface of two GS subunits within two hexameric rings. The observed correlation between GS assembly facilitated by 2-OG and its catalytic activity is substantiated by structural reorientations at the GS-GS interface, confirming the previously reported phenomenon of "funnel activation" in GS. However, the authors did not present the cryo-EM structure of M. mazei GS in complex with ATP and glutamate in the presence of 2-OG, which could have shed light on the differences in glutamine biosynthesis between previously reported GS enzymes and the 2-OG-bound M. mazei GS.

Furthermore, besides revealing the cryo-EM structure of 2-OG-bound GS, the study also observed the filamentous form of GS, suggesting that filament formation may be a universal stacking mechanism across archaeal and bacterial species. However, efforts to enhance resolution to investigate whether the stacked polymer is induced by 2-OG or other factors such as ions or metabolites were not undertaken by the authors, leaving room for further exploration into the mechanisms underlying filament formation in GS.

We thank Reviewer #2 for the detailed assessment and valuable input. We will address those comments in the updated manuscript and clarify the message.

(1) The discrepancy of the dodecamer formation (max. at 5 mM 2-OG) and the enzyme activity (max. at 12.5 mM 2-OG). We assume that there are two effects caused by 2-OG: 1. cooperativity of binding (less 2-OG needed to facilitate dodecamer formation) and 2. priming of each active site. See also Reviewer #1 R.1). We assume this is the reason why the activity of dodecameric GlnA1 can be further enhanced by increased 2-OG concentration until all catalytic sites are primed.

(2) The lack of the structure of a 2-OG and ATP-bound GlnA1. Although we strongly agree that this would be a highly interesting structure, it seems out of the scope of a typical revision to request new cryo-EM structures. We evaluate the findings of our present study concerning the 2-OG effects as important insights into the strongly discussed field of glutamine synthetase regulation, even without the requested additional structures.

(3) The observed GlnA1-filaments are an interesting finding. We certainly agree with the referee on that point, that the stacked polymers are potentially induced by 2-OG or ions. However, it is out of the main focus of this manuscript to further explore those filaments. Nevertheless, this observation could serve as an interesting starting point for future experiments.

> ***Reviewer #3 (Public Review)***:
>
> *Summary:*
>
> *The current manuscript investigates the effect of 2-oxoglutarate and the Glk1 protein as modulators of the enzymatic reactivity of glutamine synthetase. To do this, the authors rely on mass photometry, specific activity measurements, and single-particle cryo-EM data.*
>
> *From the results obtained, the authors convey that glutamine synthetase from Methanosarcina mazei exists in a non-active monomeric/dimeric form under low concentrations of 2-oxoglutarate, and its oligomerization into a dodecameric complex is triggered by higher concentration of 2-oxoglutarate, also resulting in the enhancement of the enzyme activity.*
>
> *Strengths:*
>
> *Glutamine synthetase is a crucial enzyme in all domains of life. The dodecameric fold of GS is recurrent amongst prokaryotic and archaea organisms, while the enzyme activity can be regulated in distinct ways. This is a very interesting work combining protein biochemistry with structural biology.*
>
> *The role of 2-OG is here highlighted as a crucial effector for enzyme oligomerization and full reactivity.*
>
> *Weaknesses:*
>
> *Various opportunities to enhance the current state-of-the-art were missed. In particular, omissions of the ligand-bound state of GnK1 leave unexplained the lack of its interaction with GS (in contradiction with previous results from the authors). A finer dissection of the effect and role of 2-oxoglurate are missing and important questions remain unanswered (e.g. are dimers relevant during early stages of the interaction or why previous GS dodecameric structures do not show 2-oxoglutarate).*

We thank Reviewer #3 for the expert evaluation and inspiring criticism.

(1) Encouragement to examine ligand-bound states of GlnK1. We agree and plan to perform the suggested experiments exploring the conditions under which GlnA1 and GlnK1 might interact. We will perform the MP experiments in the presence of ATP. In GlnA1 activity test assays when evaluating the presence/effects of GlnK1 on GlnA1 activity, however, ATP was always present in high concentrations and still we did not observe a significant effect of GlnK1 on the GlnA1 activity.

(2) The exact role of 2-OG could have been dissected much better. We agree on that point and will improve the clarity of the manuscript. See also Reviewer #1 R.1.

(3) The lack of studies on dimers. This is actually an interesting point, which we did not consider during writing the manuscript. Now, re-analysing all our MP data in this respect, GlnA1 is likely a dimer as smallest species. Consequently, we will add more supplementary data which supports this observation and change the text accordingly.

(4) Previous studies and structures did not show the 2-OG. We assume that for other structures, no additional 2-OG was added, and the groups did not specifically analyse for this metabolite either. All methanoarchaea perform methanogenesis and contain the oxidative part of the TCA cycle exclusively for the generation of glutamate (anabolism) but not a closed TCA cycle enabling them to use internal 2-OG concentration as internal signal for nitrogen availability. In the case of bacterial GS from organisms with a closed TCA cycle used for energy metabolism (oxidation of acetyl CoA) like e.g. *E. coli*, the formation of an active dodecameric GS form underlies another mechanism independent of 2-OG. In case of the recent *M. mazei* GS structures published by Schumacher et al. 2023, the dodecameric structure is probably a result from the heterologous expression and purification from *E. coli*. (See also Reviewer #1 R.2). One example of methanoarchaeal glutamine synthetases that do in fact contain the 2-OG in the structure, is Müller et al. 2023.

> ***Recommendations for the authors:***
>
> ***Reviewer #1 (Recommendations For The Authors):***
>
> *Specific issues:*
>
> *L 141: 2-OG levels increase due to slowing GOGAT reaction (due to Gln limitation as a consequence of N-starvation).... (2-OG also increases in bacteria that lack GDH...)*
>
> *As the GS-GOGAT cycle is the major route of ammonium assimilation, consumption of 2-OG by GDH is probably only relevant under high ammonium concentrations.*

In Methanoarchaea, GS is strictly regulated and expression strongly repressed under nitrogen sufficiency - thus glutamate for anabolism is mainly generated by GDH under N sufficiency consuming 2-OG delivered by the oxidative part of the TCA cycle (Methanogenesis is the energy metabolism in methanoarchaea, a closed TCA cycle is not present) thus 2-OG is increasing under nitrogen limitation, when no NH3 is available for GDH.

> *L148: it is not clear what is meant by: "and due to the indirect GS activity assay"*

We apologize for not being clear here. The GS activity assay used is the classical assay by Sahpiro & Stadtman 1970 and is a coupled optical test assay (coupling the ATP consumption of the GS activity to the oxidation of NADH by lactate dehydrogenase). Based on the coupled test assay the measurements of low activities show a high deviation. We now added this information in the revised MS respectively.

> *L: 177: arguing about 2-OG affinities: more precisely, the 0.75 mM 2-OG is the EC50 concentration of 2-OG for triggering dodecameric formation; it might not directly reflect the total 2-OG affinity, since the affinity may be modulated by (anti)cooperative effects, or by additional sites... as there may be different 2-OG binding sites involved... (same in line 201)*

Thank you for the valuable input. We changed KD to EC50 within the entire manuscript. Concerning possible additional 2-OG binding sites: we did not see any other 2-OG in the cryo-EM structure aside from the described one and we therefore assume that the one described in the manuscript is the main and only one. Considering the high amounts of 2-OG (12.5 mM)

used in the structure, it is quite unlikely that additional 2-OG sites exist since they would have unphysiologically low affinities.

> *In this respect, instead of the rather poor assay shown in Figure 1D, a more detailed determination of catalytic activation by different 2-OG concentrations should be done (similar to 1A)... This would allow a direct comparison between dodecamerization and enzymatic activation.*

We agree and performed the respective experiments, which are now presented in revised Fig. 1D

> *Discussion: the role of 2-OG as a direct activator, comparison with other prokaryotic GS: in other cases, 2-OG affects GS indirectly by being sensed by PII proteins or other 2-OG sensing mechanisms (like 2OG-NtcA-mediated repression of IF factors in cyanobacteria)*

We agree and have added that information in the discussion as suggested.

> *290. Unclear: As a second step of activation, the allosteric binding of 2-OG causes a series of conformational.... where is this site located? According to the catalytic effects (compare 1A and 1D) this site should have a lower affinity ...*

Thank you very much for pointing this out. Binding of 2-OG only occurs in one specific allosteric binding-site. Binding however, has two effects on the GlnA1: dodecamer assembly and priming of the active site (with two specific EC50, which are now shown in Fig. 1A and D).

See also public comment #1 (1).

> ***Reviewer #2 (Recommendations For The Authors):***
>
> *The primary concern for me is that mass photometry might lead to incorrect conclusions. The differences in the forms of GS seen in SEC and MP suggest that GS can indeed form a stable dodecamer when the concentration of GS is high enough, as shown in Figure S1B. I strongly suggest using an additional biophysical method to explore the connection between GS and 2-OG in terms of both assembly and activity, to truly understand 2-OG's role in the process of assembly and catalysis.*

We apologize if we did not present this clear enough, however the MP analysis of GlnA1 in the absence of 2-OG showed always (monomers/) dimers, dodecamers were only present in the presence of 2-OG. The SEC analysis in Fig. S1B has been performed in the presence of 12.5 mM 2-OG, we realized this information is missing in the figure legend - we now added this in the revised version. The 2-OG is in addition visible in the Cryo EM structure. Thus, we do not agree to perform additional biophysical methods.

> *As for the other experimental findings, they appear satisfactory to me, and I have no reservations regarding the cryoEM data.*
>
> *(1) Mass photometry is a fancy technique that uses only a tiny amount of protein to study how they come together. However, the concentration of the protein used in the experiment might be lower than what's needed for them to stick together properly. So, the authors saw a lot of single proteins or pairs instead of bigger groups. They showed in Figure S1B that the M. mazei GS came out earlier than a 440-kDa reference protein, indicating it's actually a dodecamer. But when they looked at the dodecamer fraction using mass photometry, they found smaller bits, suggesting the GS was breaking apart because the concentration used was too low. To fix this, they could try using a technique called analytic ultracentrifuge (AUC) with different amounts of 2-OG to see if they can*

> *spot single proteins or pairs when they use a bit more GS. They could also try another technique called SEC-MALS to do similar tests. If they do this, they could replace Figure 1A with new data showing fully formed GS dodecamers when they use the right amount of 2-OG.*

Thank you for this input. In MP we looked at dodecamer formation after removing the 2-OG entirely and re-adding it in the respective concentration. We think that GlnA1 is much more unstable in its monomeric/dimeric fraction and that the complete and harsh removal of 2-OG results in some dysfunctional protein which does not recover the dodecameric conformation after dialysis and re-addition of 2-OG. Looking at the dodecamer-peak right after SEC however, we exclusively see dodecamers, which is now included as an additional supplementary figure (suppl. Fig. 1C). Consequently, we did not perform additional experiments.

> *(2) Building on the last point, the estimated binding strength (Kd) between 2-OG and GS might be lower than it really is, because the GS often breaks apart from its dodecameric form in this experiment, even though 2-OG helps keep the pairs together, as seen with cryoEM. What if they used 5-10 times more GS in the mass photometry experiment? Would the estimated bond strength stay the same? Could they use AUC or other techniques like ITC to find out the real, not just estimated, strength of the bond?*

We agree that the term KD is not suitable. We have changed the term KD to EC50 as suggested by reviewer #1, which describes the effective concentration required for 50 % dodecamer assembly. Furthermore, we disagree that the dodecamer breaks apart when the concentrations are as low as in MP experiments. The actual reason for the breaking is rather the harsh dialysis to remove all 2-OG before MP experiments. Right after SEC, the we exclusively see dodecamer in MP (suppl. Fig. S1C). See also #2 (1).

> *(3) The fact that the GS hardly works without 2-OG is interesting. I tried to understand the experiment setup, but it wasn't clear as the protocol mentioned in the author's 2021 FEBS paper referred to an old paper from 1970. The "coupled optical test assay" they talked about wasn't explained well. I found other papers that used phosphometry assays to see how much ATP was used up. I suggest the authors give a better, more detailed explanation of their experiments in the methods section. Also, it's unclear why the GS activity keeps going up from 5 to 12.5 mM 2-OG, even though they said it's saturated. They suggested there might be another change happening from 5 to 12.5 mM 2-OG. If that's the case, they should try to get a cryo-EM picture of the GS with lots of 2-OG, both with and without ATP/glutamate (or the Met-Sox-P-ADP inhibitor), to see what's happening at a structural level during this change caused by 2-OG.*

We agree with the reviewer that the GS assay was not explained in detail (since published and known for several years). However, we now added the more detailed description of the assay in the revised MS, which also measures the ATP used up by GS, but couples the generation of ADP to an optical test assay producing pyruvate from PEP with the generated ADP catalysed by pyruvate kinase present in the assay. This generated pyruvate is finally reduced to lactate by the present lactate dehydrogenase consuming NADH, the reduction of which is monitored at 340 nm.

The still increasing activity of GS after dodecamer formation (max. at 5 mM 2-OG) and the continuously increasing enzyme activity (max. at 12.5 mM 2-OG): See also public reviews, we assume that there are two effects caused by 2-OG: 1. cooperativity of binding (less 2-OG needed to facilitate dodecamer formation) and 2. priming of each active site.

The suggested additional experiments with and without ATP/Glutamate: Although we strongly agree that this would be a highly interesting structure, it seems out of the scope of a

typical revision to request new cryo-EM structures. We evaluate the findings of our present study concerning the 2-OG effects as important insights into the strongly discussed field of glutamine synthetase regulation, even without the requested additional structures.

> *(4) Please remake Figure S2, the panels are too small to read the words. At least I have difficulty doing so.*

We assume the reviewer is pointing to Suppl. Fig S3, we now changed this figure accordingly.

> *Line 153, the reference Schumacher et al. 23, should be 2023?*

Yes, thank you. We corrected that.

> *Line 497. I believe it's UCSF ChimeraX, not Chimera.*

We apologize and corrected accordingly.

> ***Reviewer #3 (Recommendations For The Authors):***
>
> *Recent studies on the Methanothermococcus thermolithotrophicus glutamine synthetase, published by Müller et al., 2024, have identified the binding site for 2-oxoglutarate as well as the conformational changes that were induced in the protein by its presence. In the present study, the authors confirm these observations and additionally establish a link between the presence of 2-oxoglutarate and the dodecameric fold and full activation of GS.*
>
> *Curiously, here, the authors could not confirm their own findings that the dodecameric GS can directly interact with the PII-like GlnK1 protein and the small peptide sP26. However, the lack of mention of the GlnK-bound state in these studies is very alarming since it certainly is highly relevant here.*

We agree with the reviewer that we have not observed the interaction with GlnK1 and sP26 in the recent study. Consequently, we speculate that yet unknown cellular factor(s) might be required for an interaction of GlnA1 with GlnK1 and sP26, which were not present in the in vitro experiments using purified proteins, however they were present in the previous pull-down approaches (Ehlers et al. 2005, Gutt et al. 2021). Another reason might be that post-translational modifications occur in *M. mazei*, which might be important for the interaction, which are also not present in purified proteins expressed in *E. coli*.

> *The manuscript interest could have been substantially increased if the authors had done finer biochemical and enzymatic analyses on the oligomerization process of GS, used GlnK1 bound to known effectors in their assays and would have done some more efforts to extrapolate their findings (even if a small niche) of related glutamine synthetases.*

We thank the reviewer for their valuable encouragement to explore ligand-bound-states of GlnK1. However, in this manuscript we mainly focused on 2-OG as activator of GlnA1 and decided to dedicate future experiments to the exploration of conditions that possibly favor GlnK1-binding.

In principle, we have explored the ATP bound GlnK1 effects on GlnA1 activity in the activity assays (Fig. 2E) since ATP (3.6 mM) is present. GlnK1 however showed no effects on GlnA1 activity.

> *In general, the manuscript is poorly written, with grammatically incorrect sentences that at times, which stands in the way of passing on the message of the manuscript.*

> *Particular points:*
>
> *(1) It is mentioned that 2-OG induces the active oligomeric (dodecamer, 12-mer) state of GlnA1 without detectable intermediates. However, only 62 % of the starting inactive enzyme yields active 12-mers. Note that this is contradicted in line 212.*

Thanks for pointing out this discrepancy. After removing all 2-OG as we did before MP-experiments, GlnA1 doesn't reach full dodecamers anymore when 2-OG is re-added. This is not because the 2-OG amount is not enough to trigger full assembly, but because the protein is much more unstable in the absence of 2-OG, so we predict that some GlnA1 breaks during dialysis. See also answer reviewer #2 (1) and supplementary figure S1C.

> *Is there any protein precipitation upon the addition of 2-OG? Is all protein being detected in the assay, meaning, is monomer/dimer + dodecamer yields close to 100% of the total enzyme in the assay?*

There is no protein precipitation upon the addition of 2-OG, indeed, GlnA1 is much more stable in the presence of 2-OG. In the mass photometry experiments, all particles are measured, precipitated protein would be visible as big entities in the MP.

> *Please add to Figure 1 the amount of monomer/dimer during titration. Some debate why there is no full conversion should be tentatively provided.*

We agree with the reviewer and included the amount of monomer/dimer in the figure, as well as some discussion on why it is not fully converted again. GlnA1 is unstable without 2-OG and it was dialysed against buffer without 2-OG before MP measurements. This sample mistreatment resulted in no full re-assembly after re-adding 2-OG (although full dodecamers before dialysis (suppl. Fig. S1C).

> *(2) Figure 1B reflects an exemplary result. Here, the addition of 0.1 mM 2-OG seems to promote monomer to dimer transition. Why was this not studied in further detail? It seems highly relevant to know from which species the dodecamer is assembled.*

We thank the reviewer for their comment. However, we would like to point out that, although not shown in the figure, GlnA1 is always mainly present as dimers as the smallest entity. As suggested earlier, we have added the amount of monomers/dimers to Figure 1A, which shows low monomer-counts at all 2-OG concentrations (Fig.1A). Although not depicted in the graph starting at 0.01 mM OG, we also see mainly dimers at 0 mM 2-OG.

> *How does the y-axis compare to the number and percentage of counts assigned to the peaks? In line 713, it is written that the percentage of dodecamer considers the total number of counts, and this was plotted against the 2-OG concentration.*

We thank the reviewer for addressing this unclarity. Line 713 corresponds to Figure 1A, where we indeed plotted the percentage of dodecamer against the 2-OG-concentration. Thereby, the percentage of dodecamer corresponds to the percentage calculated from the Gaussian Fit of the MP-dodecamer-peak. In Figure 1 B, however, the y-axis displays the relative amount of counts per mass, multiple similar masses then add up to the percentage of the respective peak (Gaussian Fit above similar masses).

> *(3) Lines 714 and 721 (and elsewhere): Why only partial data is used for statistical purposes?*

We in general only show one exemplary biological replicate, since the quality of the respective GlnA1 purification sometimes varied (maximum activity ranging from 5 - 10 U/mg). Therefore, we only compared activities within the same protein purification. For the EC50 calculations of all measurements, we refer to the supplement.

> *(4) Lines 192-193: It is claimed that GlnK1 was previously shown to both regulate the activity of GlnA1 and form a complex with GlnA1. Please mention the ratio between GlnK1 and GlnA1 in this complex.*

We now included the requested information (GlnA1:GlnK1 1:1, (Ehlers et al. 2005); His6-GlnA1 (0.95 µM), His6-GlnK1 (0.65 µM); 2:1,4, Gutt et al. 2021).

> *It is also known that PII proteins such as GlnK1 can bind ADP, ATP, and 2-OG. Interestingly, however, for various described PII proteins, 2-OG can only bind after the binding of ATP.*
>
> *So, the crucial question here is what is the binding state of GlnK1?*
>
> *Were these assays performed in the absence of ATP? This is key to fully understand and connect the results to the previous observations. For example, if the GlnK1 used was bound to ADP but not to ATP, then the added 2-OG might indeed only be able to affect GlnA1 (leading to its activation/oligomerization). If this were true and according to the data reported, ADP would prevent GlnK1 from interacting with any oligomeric form of GlnA1. However, if GlnK1 bound to ATP is the form that interacts with GlnA1 (potentially validating previous results?) then, 2-OG would first bind to GlnK1 (assuming a higher affinity of 2-OG to GlnK1), eventually causing its release from GlnA1 followed by binding and activation of GlnA1.*
>
> *These experiments need to be done as they are essential to further understand the process. Given the ability of the authors to produce the protein and run such assays, it is unclear why they were not done here. As written in line 203, in this case, "under the conditions tested" is not a good enough statement, considering what is known in the field and how many more conclusions could easily be taken from such a setup.*

Thanks for the encouragement to investigate the ligand-bound states of GlnK1. We agree and plan to perform the suggested mass photometry experiments exploring the conditions under which GlnA1 and GlnK1 might interact in future work. In GlnA1 activity test assays, when evaluating the presence/effects of GlnK1 on GlnA1 activity, however, ATP was always present in high concentrations and still we did not observe a significant effect of GlnK1 on the GlnA1 activity.

> *(5) Figure 2D legend claims that the graphic shows the percentage of dodecameric GlnA1 as a function of the concentration of 2-OG. This is not what the figure shows; Figure 2D shows the dodecamer/dimer (although legend claims monomer was used, in line 732) ratio as a function of 2-OG (stated in line 736!). If this is true, a ratio of 1 means 50 % of dodecamers and dimers co-exist. This appears to be the case when GlnK1 was added, while in the absence of GlnK1 higher ratios are shown for higher 2-OG concentration implying that about 3 times more dodecamers were formed than dimers. However, wouldnt a 50 % ratio be physiologically significant?*

We apologize for the partially incorrect and also misleading figure legend and corrected it. Indeed, the ratio of dodecamers and dimers is shown. Furthermore, we did not use monomeric GlnA1 (the smallest entity is mainly a dimer, see Fig 1A), however, the molarity was calculated based on the monomer-mass. Concerning the significance of the difference

between the maximum ratio of GlnA1 and GlnK1: The ratio does appear higher, but this is mostly because adding large quantities of GlnK1 broadens all peaks at low molecular weight. This happens because the GlnK1 signal starts overlapping with the signal from GlnA1, leading to inflated GlnA1 dimer counts. We therefore do not think that this is biologically significant, especially as the activities do not differ under these conditions.

> *(6) Is it possible that the uncleaved GlnA1 tag is preventing interaction with GlnK1? This should be discussed.*

This is of course a very important point. We however realized that Schumacher et al. also used an N-terminal His-tag, so we assume that the N-terminal tag is not hampering the interaction.

> *(7) Line 228: Please detail the reported discrepancies in rmsd between the current protein and the gram-negative enzymes.*

The differences in rmsd between our *M.mazei* GlnA1 structure and the structure of gram-negative enzymes is caused by a) sequence similarity: E.g. *M.mazei* GlnA1 compared to *B.subtilis* GlnA have a sequence percent identity of 58.47; b) ligands in the structure: The *B.Subtilis* structure contains L-Methionine-S-sulfoximine phosphate, a transition state inhibitor, while the *M. mazei* structure contains 2OG; c) Methodology: The structural determination methods also contribute to these differences. *B. subtilis* GlnA was determined using X-ray crystallography, while the *M. mazei* GlnA1 structure was resolved using Cryo-EM, where the protein behaves differently in ice compared to a crystal.

> *(8) Line 747: The figure title claims "dimeric interface" although the manuscript body only refers to "hexameric interface" or "inter-hexamer interface" (line 224). Moreover, the figure 4 legend uses terms such as vertical and horizontal dimers and this too should be uniformized within the manuscript.*

Thank you for your valuable feedback. We have updated both the figure title and the figure legend as well in the main text to ensure consistency in the description.

> *(9) Line 752: The description of the color scheme used here is somehow unclear.*

Thanks for pointing this out. We changed the description to make it more comprehensive.

> *(10) Please label H14/15 and H14/H15ín Fig 4C zoom.*

We agree that this has not been very clear. We added helix labels.

> *(11) In Figure 4D legend, make sure to note that the binding sites for the substrate are based on homologies with another enzyme poised with these molecules.*
>
> *The same should be clear in the text: sites are not known, they are assumed to be, based on homologies (paragraph starting at line 239).*

Concerning this comment we want to point out that we studied the exact same enzyme as the Schumacher group, except that we used 2-OG in our experiments, which they did not.

> *(12) Figure 3 appears redundant in light of Figure 4.*
>
> *(13) Line 235: When mentioning F24, please refer to Figure 5.*

Thank you, we changed that accordingly.

> *(14) Please provide the distances for the bonds depicted in Figure 4B.*

Thanks for pointing this out, we added distance labels to Figure 4B. For reasons of clarity only to three H-bonds.

> *(15) Line 241: D57 is likely serving to abstract a proton from ammonium, what is residue Glu307 potentially doing? The information seems missing in light of how the sentence is built.*

Thanks for pointing this out. According to previous studies both residues are likely involved in proton abstraction - first from ammonium, and then from the formed gamma-ammonium group. Additionally, they contribute in shielding the active site from bulk solvent to prevent hydrolysis of the formed phospho-glutamate.

> *(16) Why do the authors assume that increased concentrations of 2-OG are a signal for N starvation only in M. mazei and not in all prokaryotic equivalent systems (line 288)?*

In line 288, we did not claim that this is a unique signal for *M. mazei*. It is also the central N-starvation signal in Cyanobacteria but not directly perceived by the cyanobacterial GS through binding directly to GS.

> *The authors should look into the residues that bind 2-OG and check if they are conserved in other GS. The results of this sequence analysis should be discussed in line with the variable prokaryotic glutamine synthetase types of activity modulation that were exposed in the introduction and Figure 7.*

Please refer to supplementary figure S5, where we already aligned the mentioned glutamine synthetase sequences. Since this was also already discussed in Müller et al. 2024, we did not want to repeat their observations and refer to our supplementary figure in too much detail.

> *(17) Figure 5 title: Replace TS by transition state structures of homology enzymes, or alike.*

Thank you for this suggestion. We did not change the title however, since it is not a homologue but the exact same glutamine synthetase from *Methanosarcina mazei*.

> *(18) Line 249: D170 is not shown in Figure 5A or elsewhere in Figure 5.*

Thank you for pointing this out. We added D170 to figure 5A.

> *(19) Representative density for the residues binding 2-OG should be provided, maybe in a supplemental figure.*

Thank you for the suggestion. We added the densities of 2-OG-binding residues to figure 4B

> *(20) Line 260: Please add a reference when describing the phosphoryl transfer.*

We thank the reviewer for this important point and added that accordingly.

> *(21) Line 296: The binding of 2-OG indeed appears to be cooperative, such that at concentrations above its binding affinity to the protein, only dodecamers are seen (under experimental conditions). However, claiming that the oligomerization is fast is not correct*

> *when the experimental setup includes 10 minutes of incubation before measurements are done. Please correct this within the entire manuscript.*
>
> *A (fast) continuous kinetic assay could have confirmed this point and revealed the oligomerization steps and the intermediaries in the process (maybe monomer/dimers, then dimers/hexamers, and then hexamers/dodecamers). Such assays would have been highly valuable to this study.*

We thank the reviewer for this suggestion, but disagree. It is indeed a rather fast regulation (as activity assays without pre-incubation only takes 1 min longer to reach full activity, see the newly included suppl. Fig S6). Considering other regulation mechanisms like e.g. transcription or translation regulation, an activation that takes only 60 s is actually quite quick.

> *(22) Line 305 (and elsewhere in the manuscript): the authors state that 2-OG primes the active site for a transition state. This appears incorrect. The transition state is the highest energy state in an enzymatic reaction progressing from substrate to product. Meaning, the transition state is a state that has a more or less modified form of the original substrate bound to the active site. This is not the case.*
>
> *In line 366 an "active open state" appears much more adequate to use.*

We agree and changed accordingly throughout the manuscript.

> *(23) Line 330: Please delete "found". Eventually replace it with "confirmed": As the authors write, others have described this residue as a ligand to glutamine.*

Thanks, we changed that accordingly, although previous descriptions were just based on homologies without the experimental validation.

> *(24) The discussion in at various points summarizing again the results. It should be trimmed and improved.*
>
> *(25) Line 381: replace "two fast" with "fast"?*

We thank the reviewer for this suggestion, but disagree on this point. We especially wanted to highlight that there are **two** central nitrogen-metabolites involved in the direct regulation of GlnA1, that means TWO fast direct processes mediated by 2-OG and glutamine.

https://doi.org/10.7554/eLife.97484.2.sa0